Density-Functional Molecular-Dynamics Techniques, Pseudopotential Techniques and Reduced (0-1-2) Dimensionality Working Groups

Node: **Jülich**

Re-exchange controlled Diffusion in Surfactant-mediated Epitaxial Growth: Si on As-terminated Si(111)

K. Schroeder, B. Engels, P. Richard and S. Blügel

Institut für Festkörperforschung, Forschungszentrum Jülich, D-52425 Jülich, Germany

Abstract

For a Si adatom on the Si(111) surface passivated by an As surfactant layer the adatom diffusion barrier (E_D), the exchange barrier (E_{EX}) for incorporation and the energy gain (E_B) due to incorporation into the As layer are calculated using an *ab initio* total energy and force method. We found that the activation energies for surface diffusion and exchange are similar in size and much smaller than the activation energy for the re-exchange (E_{REEX}) process ($E_D \sim E_{EX} << E_{REEX} = E_{EX} + E_B$). We propose that adatoms are rapidly incorporated into the As layer and the effective diffusion is determined by the re-exchange process.

Comment:

We have prepared the figures in this Newsletter with gnuplot in TEX-format for easy distribution. More detailed figures in postscript–format and a movie of the exchange process can be found at the following www-address:

http://www.kfa-juelich.de/iff/personen/K.Schroeder.html

Understanding, controlling and modifying the growth of nanoscale-size structures is of major importance for the design of new semiconductor quantum devices. Unfortunately, many interesting materials such as Ge/Si cannot be grown easily as multiple heterostructures with atomically flat interfaces because the strain due to lattice mismatch leads to three-dimensional (3D) islanding.

Several groups[1, 2, 3, 4] have shown that monolayer (ML) coverage of surfactants can improve the layer-by-layer growth in heteroepitaxy. For example, group-V elements (Sb, As) change the growth mode for Ge on Si(111) from 3D islands (Stranski-Krastanov growth) on clean Si(111) to 2D islands (Frank van der Merwe growth). In general, the growth of films depends on the surface free energies, kinetic effects, and the strain energy. Surfactants influence the growth in several ways: They have a low surface free energy which makes them float on the surface of the

growing crystal without being incorporated. This changes the kinetics of the surface motion and of the incorporation of deposited adatoms and leads to a modification of adatom diffusion.

The kinetics of surface processes of an adatom are not yet understood in detail. But they determine the growth mode decisively[5]: If the diffusion length of adatoms (i.e. the distance the atoms move on average before they are incorporated) is large compared to the terrace width of the crystal surface, the atoms are likely to be incorporated at a step edge. Then, the crystal grows by step-flow mode. On the other hand, if the diffusion length is much smaller than the terrace width, e.g. due to trapping at surface impurities or incorporation into a surfactant layer, growth proceeds by nucleation and growth of islands.

To get some insight into the *kinetic aspects of surfactant mediated growth* without the complication of strain, Si(111) homoepitaxy was studied. Even then, the prediction of the influence of a particular surfactant species on surface kinetics, and in particular on the diffusion length, is far from being trivial. There are two opposing effects due to surfactants: Group-V elements like As passivate the Si(111) surface due to their extra electron [for As termination this leads to an unreconstructed Si(111) surface[6]]. This tends to lower the diffusion barrier of deposited atoms and to increase the diffusion length. On the other hand, adatoms have to be incorporated under the surfactant layer eventually. Intuitively, one expects a high activation barrier for this exchange process due to the required breaking of bonds. Incorporation tends to decrease the diffusion length because the adatoms are trapped. The diffusion length is determined by the relation of the kinetic coefficients, i.e. the barrier heights, for surface diffusion and exchange, respectively. Two different scenarios of the effect of surfactants (and in particular of As) on the kinetics of adatoms have been discussed:

(i) Voigtländer *et al.* [7] have performed experiments on homoepitaxy of Si on clean and As(1 ML) covered Si(111). They find a drastic increase of the island density on the As (or Sb) covered surface and a decrease of the width of the island free (denuded) zone along step edges. They interpreted these results as a decrease of the diffusion length of Si adatoms in the presence of surfactants due to a reduction of the *effective* diffusion coefficient. From the experiment one cannot decide whether this effect is due to an increase of the diffusion activation energy on the surfactant covered surface, or whether the termination of the diffusion path by incorporation of the Si adatoms under the surfactant layer plays the decisive role.

(ii) On the other hand, Kaxiras[8, 9] assumes that deposited adatoms move rapidly across the passivated surface. He argues further that surfactants not only passivate the flat surface but also the step edges, which reduces the incorporation probability of adatoms. Thus, although in this scenario the diffusion length is much larger than the terrace width, homogeneous nucleation of islands on the terraces can take place, in spite of a high activation barrier for exchange. Kaxiras *et al.* [9] have substantiated these arguments by *ab initio* calculations for the exchange of *full monolayers* of adatoms and surfactants for which they find high energy barriers.

In this letter we investigate for the first time the barriers for all kinetic processes for single Si adatoms on a surfactant (1 ML As) covered Si(111) in a large surface supercell. We determine the equilibrium configuration of the Si adatom by minimizing the total energy of the supercell with respect to all atomic coordinates and find saddle points by restricted relaxation similar

to the "hyper-plane adaptive constraint (HAC)" method [10], i.e. by minimizing the energy subject to additional constraints. We calculate the activation energies E_D for surface diffusion, E_{EX} for incorporation of a Si adatom by exchange with an As surfactant atom, and E_{REEX} for re-exchange. We find a complex exchange path which avoids to a large extent the breaking of bonds. This leads to a surprisingly low E_{EX} which is comparable to E_D. As a consequence, we suggest a new scenario: the re-exchange controlled diffusion of Si adatoms on surfactant covered Si(111), in full agreement with experiments.

All calculations have been carried out by use of norm-conserving pseudopotentials [11] of the Kleinman-Bylander form [12] and the local density approximation [13] combined with iterative diagonalization schemes for the eigenvalue problem [14]. Force calculations combined with molecular statics [15] are used to determine the minimum energy configurations and the reaction pathways. The surface is simulated by a repeated slab model consisting of 6 atomic Si(111) layers in an inversion symmetric arrangement, 1 ML As on each Si surface, and 1 adatom on each As layer, separated by a vacuum equivalent to 6 atomic Si layers. We find that the p(3×3) periodic cell in the lateral directions, 4 $\mathbf{k}_{\|}$-points in the surface Brillouin-zone and a 13.69 Ry cut-off energy in the planewave basis set are necessary to obtain well converged results [16]. The symmetry-unrestricted geometry optimization includes all atoms except those of the 2 innermost atomic layers of the slab. To establish minimum energy configurations we converged the forces acting on the atoms to less than 0.1 mRy/a.u.

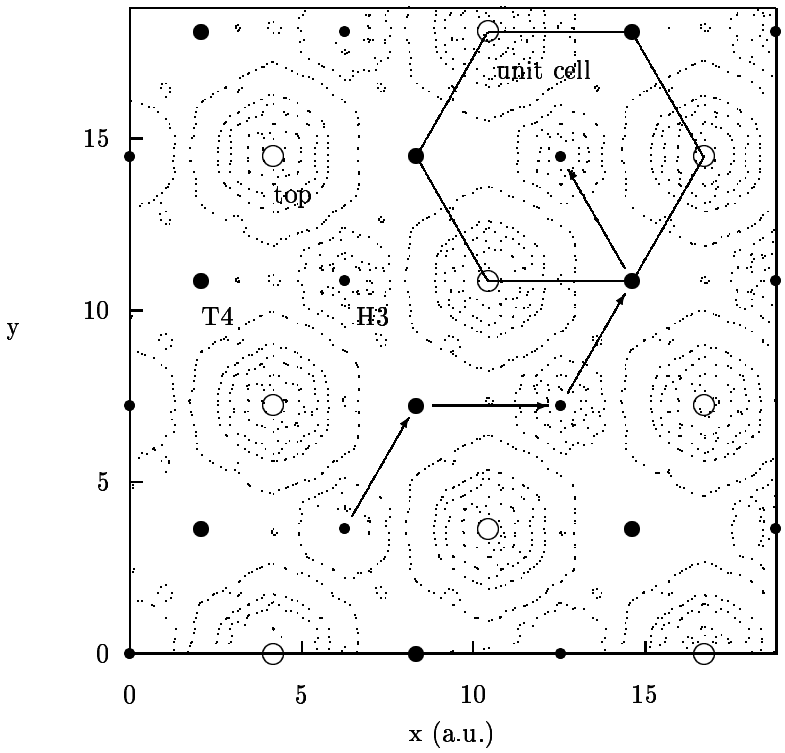

Figure 1: Energy contour for a single Si adatom above the As surfactant layer. The minima are at H3 (small full dots) and the saddle points for diffusion are at T4 (middle size full dots). The diffusion path from H3 via T4 to H3 is indicated.

Si adatom diffusion: We map out the total energy surface $E(x,y) = min_z E(x,y,z|\{\mathrm{R}\})$ by fixing the lateral position (x,y) of the Si adatom and minimizing the total energy with respect to the z-coordinate of the adatom and the coordinates of all As and Si substrate atoms {R}. Results are shown as a contour map in Fig.1. We have calculated the total energy for the Si adatom at 16 lateral positions within the irreducible triangle of the (1×1) surface unit cell of the 1 ML As covered Si(111) surface[6], including the corner points "top" (lateral position of the As top layer), T4 (1st Si layer) and H3 (3rd Si layer). We find that the equilibrium position for the Si adatom is the H3-position. The saddle point for migration into a neighboring unit cell is the T4-position, for the top-position we find the highest energy. Detailed calculations show that H3 is the only minimum and that the path H3–T4 is a trough in the energy surface. The energy difference E_D= 0.25 eV between the H3 and T4 positions is the activation energy for surface diffusion of the Si adatom on the As-layer. Compared to the diffusion on the clean Si(111) (7×7) surface with an experimentally determined activation energy of 0.76 eV[7] diffusion is much faster. This supports the idea of passivation due to group-V surfactants. The diffusion path according to our calculation is $H3 \rightarrow T4 \rightarrow H3 \rightarrow \ldots$ in troughs of the energy surface.

We found that relaxations of the As-layer and the Si substrate layers are very important for surface diffusion. For a rigid surface (at equilibrium positions of As-passivated Si(111)) the energy difference between H3 and T4 is only about half the barrier height E_D quoted above. Relaxation lowers the energy of the H3 configuration, and thus it slows down the surface diffusion.

Energy gain due to exchange of a Si adatom with an As surfactant: We calculated the configuration and energy of an incorporated Si by relaxing a configuration with the Si atom on a substitutional site and the replaced As atom on a neighboring adatom position H3. The Si atom remains close to the substitutional site and the As adatom moves closer to the incorporated Si atom. The energy of the equilibrium configuration (Si_{Sub} + As_{Ad}) is lower than the Si adatom configuration by E_B= 0.8 eV, as one expects for a good surfactant which moves to the surface to reduce the surface free energy.

Exchange Process: The search for the saddle point on the exchange reaction path Si_{Ad}+$\mathrm{As}_{Sub} \rightarrow$ Si_{Sub}+As_{Ad} is exceedingly more complicated than for the diffusion saddle point. In principle one has to determine saddle points in a multi–dimensional configuration space spanned by the position vectors of all atoms in the supercell. One usually makes the assumption that only the coordinates of the atoms mainly involved in the transition, i.e. in our case the Si adatom and of the replaced As atom, have to be restricted and that the other atoms follow their motion. This leads to the following procedure in the spirit of the HAC-approach [10]: (i) we define starting configurations *along the direct exchange path* from the Si adatom (Si_{Ad}+As_{Sub}) to As adatom configurations (Si_{Sub}+As_{Ad}) at fractions of 1/32 of the total path length; (ii) the two exchanging atoms are allowed to relax perpendicular to the direct path-vector; (iii) all other atoms are allowed to relax freely. In this way it is possible to determine energies at configurations which are not extrema on the energy surface.

The application of the procedure just described is complicated by the existence of side minima (SM) along the exchange path which are to be expected in covalently bonded materials with directed bonds. Then one first has to determine the side minima and then apply the restricted

minimization to all partial paths between neighboring minima. We followed a multiple–step procedure: (1) determine a (preliminary) saddle point by applying the HAC–method to the direct path, (2) relax the system from close to the determined saddle point by unrestricted minimization to a minimum configuration. If this is not one of the minima already known, use the HAC–method on the partial paths between all neighboring minima starting from step (1) again. In this way, we successively map the configuration space close to the transition path and can be pretty sure to have considered all relevant minima and paths. We are particularly interested in paths with low barriers since they dominate the transition rate of a thermally activated system.

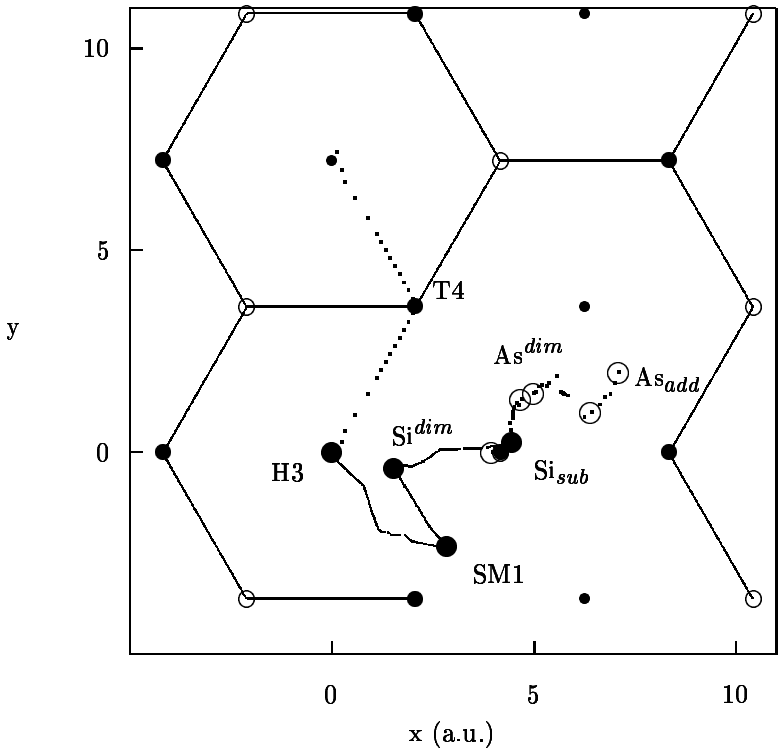

Figure 2: Positions along the exchange path projected to the surface plane. Shown are the paths of the Si atom (full line) and the As atom (dotted line) involved in the reaction. The atom positions for the local minima encountered on the path are indicated by circles (full lines for Si, dotted for As). The dashed line H3–T4–H3 is the diffusion path of the Si adatom.

The optimal path[16] is shown in Fig. 2. The coordinates along the exchange path of the two participating atoms are shown, projected to the surface of the crystal. The energy along the path is plotted in Fig. 3 vs. the path length of the Si atom. The locations of the side minima are indicated by open circles in Fig. 2 and the atomic structures of three configurations are shown in Fig. 3. One local minimum (named "dimer" configuration) is found about halfway between Si adatom and substitutional Si. It consists of a Si-As-dumbbell parallel to the surface whose center of mass is close to the top position. The energy of this dimer is approximately the same as for the Si adatom at H3. We found the barrier on the direct path from Si$_{Ad}$ to the dimer configuration to be larger than 1 eV. Thus, the system prefers a detour via a side minimum (named SM1) with a much smaller barrier of $E_{EX} = 0.27$ eV. This is the highest barrier along

the optimal exchange path. On the partial path from Si_{Ad} to SM1 the vertical height of the Si atom decreases, but only one of the 3 Si-As bonds is broken, thus leading to the moderate energy barrier. From SM1 again for energetic reasons the optimal path goes via the dimer configuration (with a low barrier of $\approx$ 0.15 eV) instead of directly towards the substitutional site (with a barrier $>$ 1 eV). On the path SM1 $\rightarrow$ dimer the coordination number of the Si and As atoms stays the same but bond angles are stretched. On the final path dimer $\rightarrow$ Si_{Sub} both atoms change their bonding partners. A barrier of $\approx$ 0.11 eV has to be overcome. The final configuration Si_{Sub}+As_{Ad} shows a 4-coordinated Si_{Sub} atom in an almost ideal tetrahedral surrounding which leads to the appreciable energy gain with E_B= 0.8 eV. We find one additional minimum (named SM3) with a lower binding energy close to the end configuration Si_{Sub}+As_{Ad}, but with the As atom at a closer (projected) distance. We checked for further side minima by full relaxation of all atoms starting from the configurations close to the saddle points of the partial paths. In each case, the system found one of the previously determined minima.

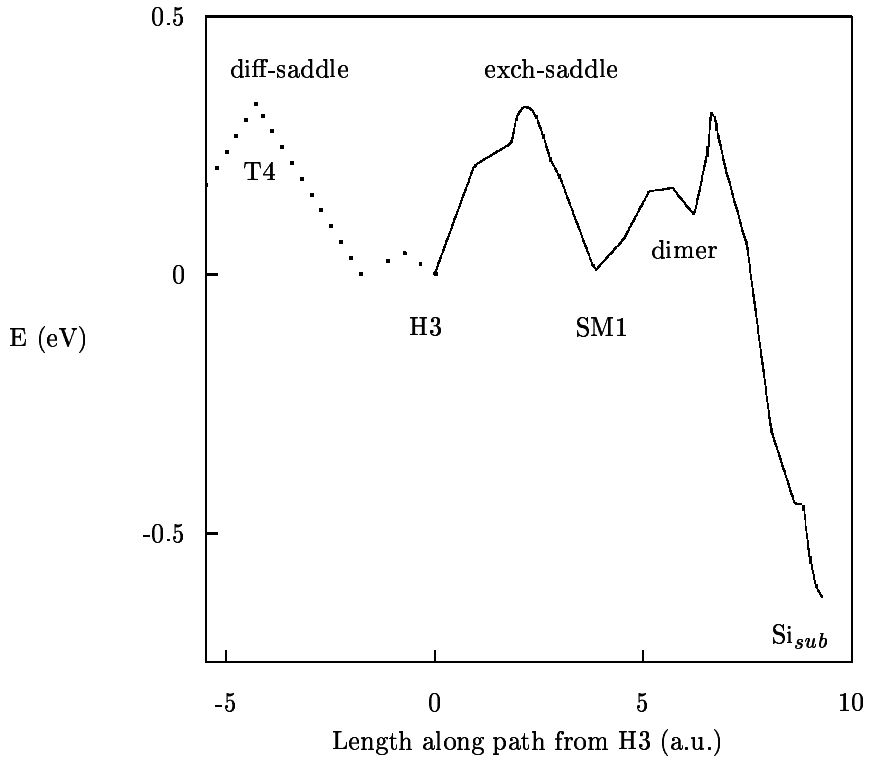

Figure 3: Energy (relative to H3 position of Si adatom) along the diffusion path (to the left of x = 0) and along the exchange path to substitutional Si (to the right). The atomic configurations for important minima are shown as insets: H3: Si_{Ad}; SM1: asymmetric dimer; Si_{Sub}: substitutional Si and As adatom (light: Si adatom; gray: As; black: Si bulk). [The insets can be found in the complete figure]

In summary, there are several local minimum configurations along the optimal exchange path. The highest barrier E_{EX} = 0.27 eV is found on the path from H3 to SM1 ("entrance channel", with the Si adatom above the As layer), the other barriers on the paths from SM1 to dimer and from dimer to SM3 ("exit channel", with the As atom above the top layer) are much smaller.

Scenario for diffusion of Si adatoms on As adlayer: In our calculation we find the following hierarchy of activation energies: $E_D = 0.25$ eV $\approx E_{EX} = 0.27$ eV $<< E_B = 0.8$ eV. Thus, the absolute minimum configuration (Si_{Sub}+As_{Ad}) can be reached immediately when diffusion is thermally activated. A newly deposited Si adatom can only make very few diffusion jumps before it is incorporated into the As-layer. Any further diffusion jump has to be thermally activated from this configuration. One possibility for a diffusion jump is to follow the exchange path backwards by re-exchange Si_{Sub}+$As_{Ad} \rightarrow Si_{Ad}$+$As_{Sub}$. The activation energy E_{REEX} involved in this process is $E_{REEX} = E_{EX} + E_B \approx 1.1$ eV. This is the *effective* activation energy for diffusion of the Si adatom. The jump sequence suggested by these results is Si_{Ad}(H3) $\rightarrow$ $Si_{Sub} \rightarrow \ldots \rightarrow Si_{Ad}$(H3) $\rightarrow Si_{Ad}$(H3,next cell) $\rightarrow \ldots \rightarrow Si_{Sub}$, where the transfer from one unit cell to a neighboring cell always goes via the T4 site.

Another possibility would be similar to the "kick-out" mechanism [17] found e.g. for Au in Si. The As adatom can de-bind and diffuse freely, if the binding and diffusion energies are lower than for Si adatoms. The Si atoms are re-activated for diffusion by re-exchanging with any of the freely diffusing As adatoms. The activation energy would again be E_{REEX}. No information on the binding or diffusion energy of As adatoms on the As-terminated Si(111) surface is available yet.

The calculated values for the effective diffusion energy with local re-exchange of As_{Ad} and Si_{Sub} and the relation of the exchange and "genuine" surface diffusion barriers are in accord with the experimental findings of Voigtländer *et al.* [7]. Compared to the experimentally determined activation energy on clean Si(111), $E_{D,clean} = 0.76$ eV, the *effective* diffusion barrier, E_{REEX}, is increased. The diffusion length of Si adatoms is indeed reduced due to As surfactants, because the Si atoms are trapped in the As-layer. With increasing temperatures one expects the diffusivity to go up, which leads to fewer and larger islands at higher temperatures, as found in experiments.

In this contribution we have investigated the exchange reaction of an isolated Si adatom on the Si(111) surface passivated by an As surfactant. We found a very complicated continuous exchange path, which avoids to a large extend the breaking of chemical bonds. This leads to a rather low exchange barrier which is comparable to the energy barrier for adatom diffusion. This finding is in contrast to the widely accepted and rather intuitive view that the thermally activated surface diffusion should always be (much) faster than the exchange process. We believe, the fact that the relaxation slows down the surface diffusion and at the same time lowers the exchange barrier is a general feature on covalently bonded semiconductor surfaces. Taking into account that for a good surfactant the incorporation of deposited adatoms is always energetically favorable we believe that the re-exchange dominated adatom diffusion on surfactant layers is a quite general process and may not be ignored.

References

1. M. Copel, M.C. Reuter, E. Kaxiras, and R.M. Tromp, Phys. Rev. Lett. **63**, 632 (1989).

2. M. Horn-von Hoegen *et al.*, Phys. Rev. Lett. **67**, 1130 (1991).

3. G. Meyer, B. Voigtländer, and N.M. Amer, Surf. Sci. **272**, L541 (1992).

4. B. Voigtländer and A. Zinner, J. Vac. Sci. Technol. A **12**, 1932 (1994).

5. J. Tersoff, A.W. Denier van der Gon, and R.M. Tromp, Phys. Rev. Lett. **72**, 266 (1994).

6. J.R. Patel, J.A. Golovchenko, P.E. Freeland, and H.–J. Gossmann, Phys. Rev. B **36**, 7715 (1987).

7. B. Voigtländer, A. Zinner, Th. Weber, and H.P. Bonzel, Phys. Rev. B **51**, 7583 (1995).

8. E. Kaxiras, Mat. Sci. and Engin. B **30**, 175 (1995).

9. D. Kandel and E. Kaxiras, Phys. Rev. Lett. **75**, 2742 (1995).

10. J.J. Mortensen, Y. Morikawa, B. Hammer, and J.K. Norskov, J. of Catalysis **169**, 85 (1997).

11. D. Vanderbilt, Phys. Rev. B **32**, 8412 (1985).

12. L. Kleinman, D.M. Bylander, Phys. Rev. Lett. **48**, 1425 (1982).

13. S.H. Vosko, L. Wilk, and M. Nusair, Can. J. Phys. **58**, 1200 (1980).

14. J.L. Martins and M.L. Cohen, Phys. Rev. B **37**, 6134 (1988). A more detailed description of our method will be given elsewhere.

15. R.Fletcher, *Practical Methods of Optimization* , John Wiley & Sons, 1987.

16. The equilibrium and saddle point configurations were re-calculated with a cut-off energy of 9 Ry using 4 $\mathbf{k}_{\|}$-points and 9 $\mathbf{k}_{\|}$-points, as well as for thicker slabs of 12 layers, relaxing 10 layers. The atomic configurations do not change much with the size of the basis set, although the relative energies differ. We estimate the calculated total energy differences to be correct to approximately 0.05 eV. For the determination of the entire path we used a basis set with E_{cut}= 9 Ry and 4 $\mathbf{k}_{\|}$-points.

17. U. Gösele, W. Frank, and A. Seeger, Appl. Phys. **23**, 361 (1980).

Density-Functional Molecular-Dynamics Techniques Working Group

Nodes: **Antwerp and Lisbon**

Hightligths of collaboration in the framework of the Ψ_k network

Ab-initio calculations for $AsNCa_3$ at high pressure

P.R. Vansant, P.E. Van Camp, V.E. Van Doren and J.L. Martins*

Department of Physics, University of Antwerpen (RUCA),

Groenenborgerlaan 171, B-2020 Antwerpen, Belgium

**INESC, Rua Alves Redol 9, P-1000 Lisboa CODEX, Portugal; Instituto*

Superior Tecnico, Avenida Rovisco Pais 1, P-1096 Lisboa, Portugal.

A structural optimization at constant pressure based on a variable-cell-shape scheme [1] is applied to $AsNCa_3$. The scheme minimizes the enthalpy also as function of the metric g_{ij} and of the positions of the atoms.

The structure of $AsNCa_3$ was found experimentally (see Ref. [2]) to be a distorted cubic perovskite structure which has a primitive orthorhombic (*Pbnm*) symmetry. Also theoretically the lattice parameters and internal structural parameters (existing due to the distortion) were determined and correspond within less than 1% to the experimental data.

The pressure dependence of the structure is determined by considering the difference in enthalpy $(H - H_c)$ between the considered structure and the cubic perovskite structure consisting of 5 atoms (SC5) as function of the pressure (see figure). When increasing the pressure the orthorhombic structure becomes more stable in comparison with the SC5 cubic structure. However, starting from a pressure of about 60 GPa another cubic phase SC15 consisting of 15 atoms is found to have a lower enthalpy. At this pressure a phase transition to this SC15 structure might occur. The nitrogen is then surrounded by *eight* calcium atoms as closest neighbours instead of *six* in the orthorhombic structure.

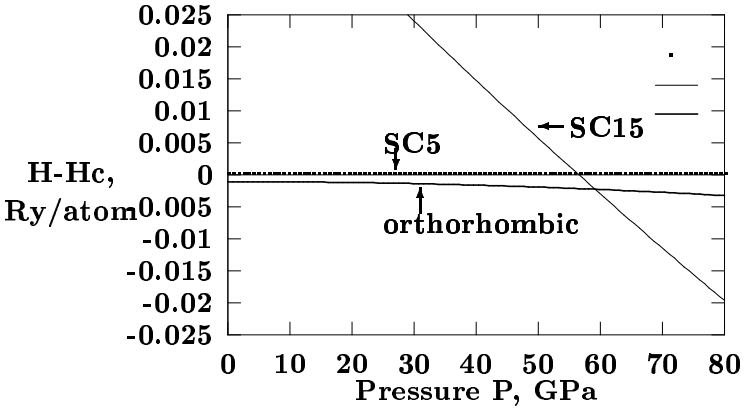

Such a SC15-like structure could also be a possible phase of $MgSiO_3$ in the earth's lower mantle.

For the orthorhombic structure a decrease of the bandgap is found with increasing pressure. The bandgap energies are 0.87 eV, 0.54 eV, 0.28 eV , 0.10 eV and 0.003 eV for respectively 0 GPa, 15 GPa, 30 GPa, 45 GPa and 60 GPa. Because LDA-calculations could give up to 50% smaller bandgaps in comparison with the correct one, a scissors-operator could be applied to obtain fairly good estimates of the bandgap energies at all those pressures. The $AsNCa_3$ compound in the orthorhombic phase is not yet metallic at 60 GPa. The SC15 structure, however, is already metallic at the moment this structure becomes more favourable in enthalpy.

Acknowledgement

This work is supported by the Belgian NSF (FWO) under grant No. 9.0053.93 and partly by the HCM network "Ab-initio Calculations of Complex Processes in Materials" grant No. ERBCHRXCT930369.

References

[1] I. Souza and J.L. Martins; submitted to Phys. Rev. B.

[2] M. Chern, D. Vennos and F. Disalvo, J. Sol. Stat. Chem. **96**, 415-425 (1992); M. Chern, F. Disalvo, J. Parise and J. Goldstone, J. Sol. Stat. Chem. **96**, 426-435 (1992).

Structural Phase Transitions of Lithium Pnictides under Pressure

P.E. Van Camp and V.E. Van Doren

Department of Physics, University of Antwerpen (RUCA),

Groenenborgerlaan 171, B-2020 Antwerpen, Belgium

The lithium pnictides, Li_3X with X=N, P, As, or Sb, are superionic conductors that have been studied before because of their potential use as electrolytes in solid state batteries. Experimentally, Li_3N is found to have the hexagonal D^1_{6h} structure (with one molecule per cell) and to undergo a phase transition at 0.42 GPa [1] or at 0.6 GPa [2] to another hexagonal structure (D^4_{6h}) with two molecules per cell. Upon releasing the pressure the D^4_{6h}- structure remains sta-

ble at zero pressure. This means that at zero pressure both hexagonal structures coexist. No other transitions are observed to a pressure of 8 GPa [2]. Both Li_3P and Li_3As are found in the D^4_{6h}-structure and no transitions were observed as yet.

In the present work we calculate the total energy at different pressures of Li_3N, Li_3P and of Li_3As in the D^1_{6h}-, D^4_{6h}- and the T^1_d-structure. The last structure (which has four molecules per cell) is included because it is the structure of the related compound Li_3Bi. The calculations are performed in the framework of the local density approximation and using ultra-soft pseudopotentials [3] and a large plane wave basis (kinetic energy cut-off of 100 Ry). For the exchange-correlation part we use the Ceperley-Alder expression [4] as parametrized by Perdew and Zunger [5]. The optimization of the lattice parameters and of the internal parameters is performed with the Broyden-Fletcher-Goldfarb-Shanno-algorithm [6]. The calculated total energies are then fitted to the third-order Birch [7] equation of state from which the bulk modulus and its pressure derivative are determined.

The calculated and experimental lattice constants (in Å), bulk moduli (in GPa) and their pressure derivatives for Li_3N are given in the table. In all cases the calculated ground state turns out to be in the D^4_{6h}- structure. Because the atomic volume in the D^1_{6h}-structure is larger than that of the D^4_{6h}-structure the calculated transition between the two structures is at a negative pressure (for Li_3N -1.1 GPa with a volume increase of 23% and an energy difference at the transition of only 16 meV/atom). The transition from D^4_{6h} to T^1_d is found at 37.9 GPa, with a volume decrease of 8% and an energy difference at the transition of 109 meV/atom. For Li_3P the transition between the two hexagonal structures is at -4.1 GPa with a volume increase of 31% and an energy difference at the transition of 174 meV/atom. For Li_3As these values are respectively -3.8 GPa, 31% and 183 meV/atom.

		Present work	Hartree-Fock [8]	Exp. [9]
D^1_{6h}	a	3.508	3.61	3.648
	c	3.745	3.84	3.873
	c/a	1.0674	1.0637	1.062
	B_0	61.02	-	-
	B_0'	3.7	-	-
D^4_{6h}	a	3.418	-	-
	c	6.100	-	-
	u	0.5776	-	-
	c/a	1.7846	-	-
	B_0	78.166	-	-
	B_0'	3.77	-	-
T^1_d	a	4.824	-	-
	B_0	82.75	-	-
	B_0'	3.84	-	-

Acknowledgement

This work is supported by the Belgian NSF (FWO) under grant No. 9.0053.93 and partly by the HCM network "Ab-initio Calculations of Complex Processes in Materials" grant No. ERBCHRXCT930369.

References

[1] M. Mali, J. Roos and D. Brinkmann, Phys.Rev. **B36**, 3888 (1987).

[2] H.J. Beister, K. Syassen and J. Klein, Z.Naturforsch. **45b**, 1388 (1990).

[3] N. Troullier and J.L. Martins, Sol. Stat. Comm. **74**, 613 (1990); Phys.Rev. **B43**, 1993 (1991).

[4] D. Ceperley and B. Alder, Phys. Rev. Lett. **48**, 566 (1980).

[5] J.P. Perdew and A. Zunger, Phys. Rev. **B23**, 5048 (1981).

[6] J. Olsen and P. Jorgensen, J. Chem. Phys. **77**, 6109 (1982).

[7] F. Birch, J. Geophys. Res. **83**, 1257 (1978).

[8] M. Seel and R. Pandey, Int. J. Quant. Chem. Symp. **25**, 461 (1991).

[9] G. Nazri, Mater. Res. Soc. Symp. Proc. **135**, 117 (1989).

Node: **Helsinki**

Scientific Highlight

A major research topic in the node's activities has been the first-principles simulation of defect-related phenomena in semiconductors, both in silicon and in II-V and II-VI compound materials. Both native and introduced defects profoundly affect the electronic and optical properties of semiconductors, both as bulk materials and in engineered structures, such as superlattices and heterostructures. As there is a strong coupling between the ionic and electronic degrees of freedom, sophisticated numerical and theoretical techniques are required for predictive calculations of the defect-related properties.

Defects play a central role in semiconductor doping, as complexes formed by the dopants and by point defects (vacancies, interstitials) govern the compensation of carriers and determine the doping limits. Large lattice relaxations transform shallow levels to deep ones in the semiconducting gap. Another typical feature are the metastabilities associated with several defect complexes, especially in compound semiconductors.

Specific projects carried out recently include

(i) metastable defects in GaAs: extension of the DX and EL2 concepts
(ii) doping of ZnSe: self-compensation and carrier limits
(iii) band offsets at GaAs/ZnSe interfaces
(iv) antisite defects in SiC
(v) defects, oxygen and broadband luminescence in GaN and AlN
(vi) amorphisation of Si by ion irradiation
(vii) oxygen clusters in Si

The node works in close collaboration with companies active in the semiconductor area, such as Okmetic Ltd (major manufacturer of Si wafers) and Semitronic Ltd (SiC growth). The results and information obtained through the Network activities have benefited also the collaboration projects with industry.

For further information and complete publication lists, please consult the node's WWW page:

http://www.fyslab.hut.fi/

Node: **Lyngby**

Scientific Highlights

The Center for Atomic-scale Materials Physics (CAMP) at the Department of Physics, The Technical University of Denmark, consists of about 25 researchers including PhD students and Postdocs. The research has been in fundamental aspects of materials physics and surface physics with a particular emphasis on:

1) Metal on metal growth – including studies of surface alloy formation, segregation and elementary diffusion process by DFT and simulations of dynamics and kinetics using molecular dynamics and kinetic Monte Carlo methods based on semi-empirical interatomic potentials of the effective medium type.

2) Nano-structures and interfaces – including studies of metallic point contacts, nano-tribology, interface structures, and the magnetic, electrical, and mechanical properties of nano-structured materials.

3) Chemical properties of surfaces – including studies of adsorption, and further reactions on transition metal and semiconductor surfaces. Models have been developed on this basis describing the electronic factors of a surface determining the reactivity.

The group has benefitted from the network mainly through the newsletter and participation in the Network Conference in Schwäbisch Gmünd. The group has a number of collaborations with members of the Network and, very importantly, with experimentalists and industry.

Pseudopotential Techniques and Density-Functional Molecular-Dynamics Techniques Working Groups

Node: **Cambridge**

Simulations related to the mechanical deformation of materials

A fundamental understanding of the mechanical properties of solids is difficult because two length scales are involved simultaneously, the atomistic scale and the mesoscopic scale of elastic strain. The jointly sponsored Network/CECAM workshop was directed at the problem of bridging the gap between these two length scales. Small ab initio calculations can determine parameters which can be fed into simulations on the larger mesoscopic scale.

The research was started in Cambridge by G. Francis with calculations of the structure of grain boundaries in germanium as an example of a strongly covalently bonded material. A tilt boundary was found to have one more or less unique structure with much lower energy than any other, while a twist boundary had many different structures of roughly equal energy.

Francis then carried out simulations in which one grain was slid over the other at the grain boundary, using the germanium twist boundary. These were then extended by Carla Molteni. The first result was that sliding proceeds by a series of stick/slip processes, i.e. the bonds across the boundary would be increasingly strained until there was a sudden topological rearrangement of the bonding. The sliding was therefore discontinuous, with the energy and stress building up to a maximum until the 'click' of the rebonding. The second finding was that the rebonding occurred over only a small region of the boundary. It is not clear that would be possible in a simple 2-dimensional model with a boundary line, but it is in 3 dimensions. In a typical case only two bonds were detached from two atoms and swapped around. The third result was that the configurational path did not reverse if after some distance one reversed the direction of slide. Also as one continued, the surface got increasingly disordered with the disordered region growing in width. Both of these are indications of irreversibility and energy dissipation. Fourthly Molteni was able to work out the displacement path of the atoms during rebonding and thus the energy barrier at various stages of the sliding before the spontaneous 'click' at zero Kelvin when the barrier has gone to zero. At non-zero temperature the rebonding would occur with a probability given by a Boltzmann factor before the 'click'. In this way the relation between stress and strain rate was calculated, based on one typical rebonding which was investigated in detail. Fifthly the behaviour of 'gap states' in the semiconductor band gap was noted. The electronic structure of semiconductors with defects is often discussed in terms of gap states, the notion being that atomic relaxations are driven or accompanied by suppressing states in the band gap and driving them into the valence or conduction band, particularly the valence band. This was indeed observed at the 'click'.

At the same time V. Deyirmenjian carried out ab initio simulations of pulling a specimen of aluminium apart, containing an array of defects in the form of lines of vacancies. These were intended to be somewhat like microcracks, the computing resources not allowing anything more realistic. The intention was to see how the break-up proceeded from the defects. Deformation started by creating what could be described as a dislocation, but the atoms flowed rather smoothly over one another in a way more reminiscent of a fluid than how one might envisage a crystal.

Another aspect of that research project was to compare the ab initio results with those obtained using traditional empirical classical potential models of the interatomic bonding, such as the pairwise Morse potential and the Sutton-Chen 'glue' model. The Morse potential gave qualitatively completely wrong behaviour, while the 'glue' model gave also a type of flow movement but not quantitatively correct even when the parameters of the 'glue' model had been tuned to the properties of our computational aluminium. There were systematic deviations particularly at large strains, and an idea of our collaborator Professor M. Finnis was able to improve that significantly. The conclusion is that if it is sufficient to have some sort of ductile behaviour, then a Sutton-Chen model as modified by Finnis can give it, but that ab initio calculations are required for more accurate results pertaining to a specific metal.

In order to compare the grain boundary sliding in a ductile metal with that in the covalently bonded germanium, Molteni carried out analogous simulations on a twist and a tilt boundary of aluminium. In the one case the sliding was completely smooth and reversible with no stick/slip 'clicks'. The atoms just flowed over each other, reminiscent of the behaviour observed by Deyirmenjian noted above. In the other boundary there were some stick/slip 'clicks' but the energy jumps were an order of magnitude smaller than in the case of germanium. In a third simulation, the smoothly flowing boundary was taken and one atom removed to form a vacancy. This was found to be an 'irritant' in the boundary and the sliding was no longer smooth, ie it had developed stick/slip jumps when configurations of atoms got hung up around the vacancy. Here one grain seemed to roll over the other, with a group of three atoms rotating as a whole like a wheel– a rather bumpy triangular wheel but the adaptable flowing could cope with that. What matters in metallic bonding of an sp-bonded element like aluminium is that the local volume around an atom is nearly constant in order to accommodate the valence electron gas; but with the ionic radius only half of the atomic radius, the spatial arrangement of the nearest neighbours is less important. The sideways migration of the boundary was also observed.

All the above results concern clean boundaries without impurities. However impurities affect grain boundaries substantially, as shown for example by measurements in the group of Professor Gust in Stuttgart on grain boundaries of aluminium containing a very small bulk concentration of order 20 ppm of gallium. It was found that such small concentrations increased the grain boundary mobility by about a factor of ten. Gallium is a notorious embrittler of aluminium, but that may be a different phenomenon because it appears to involve high concentrations of gallium being sucked into the grain boundaries. Simulations were carried out on a $\sigma = 11$ (113) tilt boundary containing from zero to two monolayers of gallium. This boundary is a partic-

ularly well fitting boundary, with the environment of each atom not differing very much from that in bulk aluminium as regards the number and distances of the near neighbour atoms. Consequently the boundary energy is rather low compared with other less well fitting boundaries such as obtained in the sliding simulations of Molteni. The only local strain in the boundary is between two atoms that straddle the boundary, whose separation is 0.15 $\mathring{A}$ smaller than the nearest neighbour distance in bulk aluminium. When gallium atoms are substituted in those sites, the structure relaxes with substantial reduction in energy and a reduction in that interatomic distance to what it is in pure gallium. However it must not be thought that gallium is just a smaller atom than aluminium; in solid solution gallium has almost exactly the same atomic volume as aluminium, and in the pure state even a 10 percent larger one. Detailed results were obtained on the energetics of boundaries with 10 different concentrations of gallium, on the relaxations in the boundaries, the looseness of the atoms as measured by restoring force constants for displacements, and the energy barrier for boundary migration. These could all be explained in terms of the 'two radii' behaviour of atoms in such systems. The 'volume radius' determines the volume per atom needed to accommodate the conduction electron gas, which energetically is the stronger force. The 'near-neighbour' radius gives then the preferred near neighbour distance at that atomic volume, which depends on the crystal structure. In aluminium the two radii are nearly equal, but in gallium the near-neighbour radius is significantly smaller, which accounts for its unusual crystal structure. In the aluminium grain boundary the gallium impurities allow the relaxation of the particularly tight contact. The observed energy lowering can be more or less completely ascribed to a reduction in local strain energy. From this picture one can predict more significant effects in less well fitting boundaries including the build up of a fraction of a monolayer in thermodynamic equilibrium at room temperature. The mobility of the boundary is enhanced because gallium atoms in the boundary can more easily slide past other atoms because of the smaller near-neighbour radius while the structure is held open by the larger volume radius.

So far computational limitations have prevented any sliding calculations with impurities, but simulations involving a dislocation interacting with a grain boundary are planned. That is a more important process in plastic deformation of materials than the grain boundary sliding.

The above calculations are obviously still a long way from answering what happens in real macroscopic deformations, but they have demonstrated some of the variety of processes occurring at the atomic level and the kind of calculations that are now possible.

References

V.B. Deyirmenjian, V. Heine, M.C. Payne, V. Milman, R.M. Lynden-Bell, and M. Finnis,
Ab-initio Atomistic Simulation of the Strength of Defective Aluminum and Tests of Empirical Force Models,
Phys. Rev. B **52**, 15191-15207 (1995).

V.B. Deyirmenjian, V. Heine, M.C. Payne, V. Milman and M.W. Finnis,
Improved representation of metallic bonding in atomistic simulations,
Phil. Mag. Letters **73**, 39-44 (1996).

C. Kruse, M.W. Finnis, J.S. Lin, V.Y. Milman, M.C. Payne, A. De Vita, and M.J. Gillan,
'First principles study of the atomistic and electronic structure of the Niobium/α-Alumina(0001) interface',
Phil. Mag. Lett. **73** 377-383 (1996).

C. Molteni, G.P. Francis, M.C. Payne and V. Heine,
First principles simulation of grain boundary sliding,
Phys. Rev. Lett. **76**, 1284 (1996).

C. Molteni, G.P. Francis, M.C. Payne and V. Heine,
Temperature and strain rate effects in grain boundary sliding,
in Mat. Res. Soc. Symp. Proc. *Materials Theory, Simulations, and Parallel Algorithms*, vol. **408**, pp 277-282, E. Kaxiras, J. Joannopoulos, P. Vashishta, R.K. Kalia eds. (MRS, Pittsburgh 1996).

C. Molteni, N. Marzari, M.C. Payne and V. Heine,
Sliding mechanisms in aluminium grain boundaries,
Phys. Rev. Letters **79**, 869-872 (1997).

M.C. Payne, G.P. Francis, C. Molteni, N. Marzari, V. Deyirmenjian and V. Heine,
Ab initio investigation of grain boundary sliding,
in Mat. Res. Soc. Symp. Proc. *Materials Theory, Simulations, and Parallel Algorithms*, vol. **408**, pp. 283-289, E. Kaxiras, J. Joannopoulos, P. Vashishta, R.K. Kalia eds. (MRS, Pittsburgh 1996).

D.I. Thomson, V.Heine, M.W. Finnis and N. Marzari,
Ab-initio computaional study of Ga in an Al grain boundary,
Phil. Mag. Letters 76, 281-287 (1997).

D.I. Thomson, V. Heine, M.C. Payne, N. Marzari and M.W. Finnis,
Insight on gallium behaviour in Al grain boundaries from calculation on a σ=11 (113) boundary,
Acta Metallurgica et Materiala (submitted Aug. 1997).

Muffin tin techniques Working Group

Node: **Strasbourg**

Highlight of the results obtained with the TB-LMTO code

O. Elmouhssine, P. Krüger, G. Moraitis[1], M. A. Khan,
H. Dreyssé, J. C. Parlebas and C. Demangeat
Institut de Physique et Chimie des Matériaux (IPCMS-GEMME)
UMR 46 du CNRS-Université Louis Pasteur, 23 rue du Loess, 67037 Strasbourg Cedex, France

J. Izquierdo and A. Vega
Departamento de Fisica teorica y Nuclear, Universidad de Valladolid
47011 Valladolid, Spain

F. Amalou, H. Bouzar and M. Benakki
Département de Physique, Université de Tizi-Ouzou, Algérie

A. Mokrani
Groupe de Physique du Solide pour l'Electronique,
Université de Nantes, 2, rue de La Houssinière, 44072, Nantes, France

(December 10, 1997)

The course "Hands-on TB-LMTO computer program" was announced in the April issue (1994) of the HCM Newsletter. Two members of the theoretical group: G. Moraitis (professor) and A. Vega (post-doc from Valladolid) have registered and both of them have attended the course organized by Ove Jepsen on October 24-28, 1994, at the Max-Planck Institute in Stuttgart. Back from Stuttgart, G. Moraitis has used the code for spectroscopic and theoretical investigations of sub-stoichiometric Ti-nitrides, Ti-carbonitrides, and band structures of CoRh, CoRu, Co_3Pt alloys.

Also, calculations concerning "Spin-flop transition in Fe_nCr_m superlattices" [1] have shown the sensitivity of the Fe/Cr interface coupling with the lattice parameter. O. Elmouhssine and P. Krüger have been strongly involved in calculations concerning the adsorption of very thin films (of the monolayer range) of transition metals on metallic, or graphitic substrates. The Ph.D. thesis of Elmouhssine (April 1998) will contain the following results:

i) p(2x2) versus c(2x2) configurations for one Mn monolayer on Fe(001) [2]. This contribution shows clearly that besides the well known c(2x2) configuration, almost degenerate and more complex configurations are present and may explain the controversial XMCD results obtained by different experimental groups;

[1] present address: Département de Physique, Université de Ouagadougou, Burkina Faso

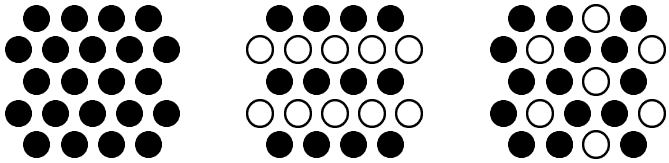

Figure 4: Magnetic configurations considered for the $3d$ transition metal monolayers on graphite (0001). Full and open circles represent up and down spins, respectively.

ii) Similar configurations are shown to be present for Mn monolayer on Co(001). These results are not in complete agreement with recent XMCD results of O'Brien and Tonner but can explain MOKE results [3];

iii) Complex magnetic configurations have been detected by O'Brien and Tonner for $Fe_n/Co(001)$. Those layered antiferromagnetic configurations [4] are shown to be present when n $\geq$ 3;

iv) Growth, structural stability, electronic structure and magnetism of MnAg(001) surface alloys [5, 6];

P. Krüger (Ph.D. thesis in January 1998) has used the TB-LMTO code for the following studies on transition metal monolayers (ML) deposited on the graphite surface:

(i) $4d$ transition metal ML [7, 8] have been investigated in an epitaxial structure, which is compatible with the experimental findings for the Ru/C(0001) system. It is found that only Ru and Rh ML can be ferromagnetic for metal-graphite interlayer distances above 2.5 Å. Due to the highly anisotropic hybridization with the C p_z orbitals, the moments depend strongly on the the adsorption site.

(ii) For the $3d$ transition metal ML [9] three magnetic configurations have been compared (see fig. 4 and table 1).

We find that the V and Cr ML are nonmagnetic, while the Fe, Co and Ni ML are ferromagnetic on graphite. For the Mn ML, the antiferromagnetic and ferrimagnetic configurations are degenerate and more stable than the ferromagnetic one. The absence of magnetic solutions for the adsorbed Cr ML can be related to the great sensitivity of Cr to frustration of the nearest neighbour coupling, which is important for the hexagonal lattice. For the unsupported Cr ML, the antiferromagnetic and a ferrimagnetic configuration exist, but they are almost degenerate with the nonmagnetic solution. By comparison with the free standing ML, we find that the graphite–metal interaction substantially reduces the magnetic moments of the adsorbed ML.

More recently, F. Amalou, a Ph.D. student registrated at the University of Tizi-Ouzou (Algeria) has started a thesis on the determination of the magnetic configurations at the surfaces of FeCr and FeRh alloys [10].

M. M. Schwickert et al (Phys. Rev. B, in press) have depicted through MOKE an oscillatory period in the interlayer exchange coupling in Fe_5V_m superlattices: within a collaboration with Valladolid we have performed calculations for both Fe_5V_m superlattices and for V_m thin films on Fe(001) and Fe(011) [11].

		Cr		Mn		Fe		Co		Ni	
		free	ads	free	ads	free	ads	free	ads	free	ads
Fo	μ	–	–	3.0	1.0	2.7	2.1	1.9	1.3	0.4	0.3
	$-E_M$	–	–	6	2	41	9	25	5	1	0.5
AF	$\|\mu\|$	1.5	–	3.1	1.9	2.5	1.2	1.4	–	–	–
	$-E_M$	0	–	33	6	29	3	7	–	–	–
Fi	μ_1	1.6	–	3.2	1.9	–	–	–	–	–	–
	μ_2	-2.2	–	-2.8	-2.0	–	–	–	–	–	–
	$-E_M$	1	–	27	6	–	–	–	–	–	–

Table 1: Magnetic moments (in units of μ_B) and magnetic energies (E_M, in units of mRy) of the different solutions of the $3d$ transition metal monolayers on graphite (0001). Fo, AF, Fi, free, and ads means ferromagnetic, antiferromagnetic, ferrimagnetic configuration (see fig 4), unsupported monolayer, and on graphite adsorbed monolayer, respectively. In the ferrimagnetic solutions, μ_1 (μ_2) is the moment of the majority (minority) type of atoms.

The node greatly appreciated and benefited from the HCM Ψ_k-Network. First the Network made possible the participation in various European conferences of senior scientists and French students which would have been almost impossible without Network's help. Another very important point is the financial support of the Network given to workshops organized by the French node. In 96 and 97 we organized three workshops supported by the Network. Once again clearly without this help, some eminent colleagues would have not been able to attend these meetings. Moreover, the collaboration with the Stuttgart node on TB-LMTO was very productive (more than 10 papers) and obviously the Network contributed greatly to the dissimenation of the TB-LMTO method and the results. We also appreciated very much the Ψ_k-Newsletter which has become a very useful tool. Finally, we would like to mention that various discussions during meetings were of great help to two members of our node in finishing a review paper published in Sur. Sci. Report on Surface and Interface Magnetism.

References

[1] G. Moraitis, M. A. Khan, H. Dreyssé and C. Demangeat, *Spin-flop transition in Fe_nCr_m superlattices*, J. Magn. Magn. Mat. **156**, 250 (1996).

[2] O. Elmouhssine, G. Moraitis, C. Demangeat and J. C. Parlebas, *p(2x2) versus c(2x2) configurations for one Mn monolayer on Fe(001)*, Phys. Rev. **B55**, R7410 (1997).

[3] O. Elmouhssine, G. Moraitis, J. A. C. Bland, C. Demangeat et al, to be published.

[4] O. Elmouhssine, A. Mokrani, G. Moraitis and C. Demangeat, *Non-ferromagnetic solutions for Fe thin films on Co(001)*, Communication at the 3rd MML'98 meeting, Vancouver, Canada, June 1998.

[5] O. Elmouhssine, G. Moraitis, J. C. Parlebas, C. Demangeat, P. Schieffer, M. C. Hanf, C. Krembel and G. Gewinner, *Relative stability of an on-top and an inverted Mn monolayer on Ag(001): Experiment and theory*, Compt. Mat. Science (1997), in press.

[6] O. Elmouhssine, G. Moraitis, J. C. Parlebas, C. Demangeat, P. Schieffer, M. C. Hanf, C. Krembel and G. Gewinner, *Growth and magnetism of one Mn monolayer on Ag(001)*, Communication to MMM-Intermag, San Francisco, January 1998.

[7] P. Krüger, A. Rakotomahevitra, G. Moraitis, J. C. Parlebas, and C. Demangeat, *Magnetism of hexagonal 4d transition metal monolayers*, Physica B **237-238**, 278 (1997).

[8] P. Krüger, J. C. Parlebas, G. Moraitis, and C. Demangeat, *Magnetism of epitaxial Ru and Rh monolayers on graphite*, Comput. Mat. Sci. (1998), in press.

[9] P. Krüger, A. Rakotomahevitra, J. C. Parlebas, and C. Demangeat, *Magnetism of hexagonal 3d transition metal monolayers on graphite*, Phys. Rev. B **57** (1998), in press.

[10] F. Amalou, H. Bouzar, M. Benakki, A. Mokrani, C. Demangeat and G. Moraitis, *Complex magnetic behavior at the surface of B2 ordered alloy*, Compt. Mat. Sc. (1997), in press.

[11] A. Vega, O. Elmouhssine, J. Izquierdo, C. Demangeat and H. Dreyssé, *The polarization map at the V/Fe interface*, submitted to Phys. Rev. B.

Scientific Highlights

The research work of our group has been devoted to the study of multicomponents metallic systems, with the purpose to understand their physical properties on the basis of *ab initio* calculations, mainly implemented within the multiple scattering framework (KKR or KKR-CPA). The work has been developed along the following lines:

1. Electronic Topological Transitions and Fermiology
2. Phase stability of metallic alloys
3. KKR-CPA and Bloch Spectral Function codes for any lattice

which will be discussed separately.

1. Electronic Topological Transitions and Fermiology

When a metallic alloy is subjected to a thermodynamic transformation (e.g. an uniaxial strain or a change of the composition) the band structure does change. As a consequence some bands at Fermi level might move up or down producing a change in the shape and the connectivity of the Fermi Surface, when the Fermi level passes across Van Hove singularities. These, since I.M. Lifshitz's 1960 paper[1], are called Electronic Topological Transitions (ETT). Lifshitz's theory shows that whenever such phenomenon occurs there is a "singular" contribution to the density of states and to the system grand potential that can be written as:

$$n(\epsilon) = n_0(\epsilon) + n_1(\epsilon) \tag{1}$$

$$\Omega = \Omega_0 + \Omega_1 \tag{2}$$

$$n_1(\epsilon) = \alpha|\epsilon - \epsilon_1|^{\frac{1}{2}}\Theta(\epsilon - \epsilon_1) \tag{3}$$

$$\Omega_1(\mu) = -\frac{4}{15}\alpha|\mu - \epsilon_1|^{\frac{5}{2}}\Theta(\mu - \epsilon_1) \tag{4}$$

where μ is the chemical potential and ϵ_1 is the energy of the Van Hove singularity. In the above equations, α is related to the effective mass of the band (assumed parabolic in a neighbourhood of ϵ_1). Ω_1 can be positive or negative depending on the kind of the Van Hove singularity and on the fact that it falls above or below the Fermi level. Accordingly, to open or close a new bit of the Fermi surface requires or releases energy. We remark that the above equations holds in absence of impurity scattering.

On the basis of the above simple arguments, one can see that on varying the concentration of a metallic solid solutions (and therefore the valence electrons per atom, in case of non homovalent

components) such "transitions" can occur, although the impurity scattering will broaden the effect of the transition. Then the transport properties will be affected, because they depend on integrals over the Fermi Surface, but also equilibrium quantities will, because of the work involved on changing the shape of the Fermi Surface.

We have studied the effects of compositional changes on the Fermi Surface topology on metallic random alloys in a review paper [2], where we also discussed the concept of Fermi surface for a disordered alloy and the technical problems connected with its numerical determination. Later, we have studied the influence of the ETT's on the equilibrium properties [3], also in presence of impurities and temperature effects, and illustrated such work for the case of Ag_cPd_{1-c} alloys [4] that present five distinct ETT's, on varying the concentration. In particular, in ref. [3] we have shown how ETT's are responsible of the deviations from Vegard's law for the atomic volume change with the concentration.

2. Phase stability of metallic alloys

The study of the phase equilibria of metallic alloys can be cast into the Density Functional theory in several ways. For instance, in order to predict the equilibrium phase of a given binary alloy, one could perform the electronic total energy calculations of many different possible phase and find out the stablest one. This procedure has several inconveniences, either due to the large amount of different possible structures for the same alloy, or to the treatment of the solid solution phase, that, unless one uses an O[N] method, as those of ref. [5, 6], requires further approximations in order to take into account the substitutional disorder.

Another inconvenience arises when one is interested in understanding the mechanisms that drive the system toward a particular phase, which is not necessarily transparent from a first principles calculation. This can be bypassed by the study of the Fermi Surface of the random phase, that often contains the seed of the ordering or phase separation occurring at low temperature [7, 8]. But, in many cases, for which the fcc Cu_cPd_{1-c} alloy is one of the most striking example, it might not be enough. In fact, in the Cu rich side of the phase diagram, such alloy orders into fcc based structures ($L1_2$), with an alternate sequence of Cu and Cu-Pd planes along the (0,0,1) direction. This ordering phenomenon, as it is well known[8], can be understood in terms of the Fermi Surface nesting mechanism, that enhances the concentration fluctuations susceptibility along the nesting direction. However, about the equiatomic composition, although the ordering occurs as an alternate sequence of Cu and Pd planes, again along the (0,0,1) direction, the equilibrium β phase has the B2 structure, i.e. geometrically a bcc rather than a fcc lattice. This implies that notwithstanding the homogeneous phase is unstable with respect to concentration waves along the (0,0,1) direction, other phenomena must occur. In the case of $Cu_{0.50}Pd_{0.50}$ an uniaxial strain of 40 percent along the (0,0,1) direction is required in order to reach the B2 phase making this problem untreatable by the perturbation theory. However, it is appealing to interpreting such Bain transition in terms of the coupling between strain and concentration fluctuations. Therefore we have chosen the route to calculate the total energy along the appropriate Bain path for alloys with superimposed concentration waves and try to get insights on the mechanisms producing the phase transformation.

Following this strategy, we have computed, by relativistic KKR and KKR-CPA methods the total energy of the equiatomic CuPd for: 1) the random alloy in the body centered tetragonal lattice; 2) the intermediate ordered alloy $(Cu_{0.75}Pd_{0.25})$-$(Cu_{0.25}Pd_{0.75})$ in the simple tetragonal lattice with two atoms per unit cell and 3) the ordered alloy again in the former lattice, varying the c/a ratio along the Bain path for all of them. In all these cases when $c/a = 1$ one gets the bcc or B2 lattices and when $c/a = \sqrt{2}$ one gets the fcc or $L1_0$ lattices.

We have found that the total energy has a function of c/a for the case 1) has two local minima corresponding to the bcc and fcc lattices separated by a relatively high energy barrier (6mRy); for the case 2) has again two local minima but the energy barrier is much lower (2mRy) and for the case 3) the $L1_0$ (fcc) lower minimum disappears and the overall lowest total energy value is taken by the B2 lattice. This suggests the following picture for the kinetics of the transformation: 1)In the random alloy phase any strain fluctuation driving toward the bcc lattice are restored by elastic forces, because the fcc local minimum is separated from the bcc minimum by the energy barrier; 2) on lowering the temperature concentration (and charge) waves occur, and the atomic diffusion in the two sublattice reduces the energy barrier; 3) the absence of the local minimum in the $L1_0$ lattice allows for a plastic deformation toward the B2 equilibrium phase.

By the analysis of the contributions to the total energy one sees that the exchange-correlation energy does not vary along the Bain path, while the equilibrium arises through a competition from the electrostatic and the band energies. The former as a minimum at the bcc-like lattices and a maximum at the fcc-like lattices, while the latter behaves exactly in the opposite way. The reason of the behaviour of the electrostatic energy is strictly related to the charge transfer, that in such systems is from Pd to Cu. The maximum charge charge transfer is in the B2 phase, a lattice quite common amongst the ionic salts, and reach the value of 0.28 electrons. We notice that in such system a concentration wave and a charge density wave are the same thing, therefore the charge transfer is directly related to the Fermi Surface nesting occurring in the random phase. But the charge transfer increases the electrostatic attraction between the Cu and Pd planes, perpendicular to the (0,0,1) direction, providing the energy to strain the lattice.

In order to complete the mechanism of this Bain transition remains to understand the reason why the band energy grows towards the B2 lattice. This is due to the applied strain that pushes the Fermi level into the Pd d-states, opening a hole pocket in the Fermi Surface. According to the ETT theory of the former section, this requires work, and this explain why the band energy favours fcc-like lattices.

The results illustrated above have been submitted recently for publication [9].

3. KKR-CPA and Bloch Spectral Function codes for any lattice

In order to perform the calculations described above, within the KKR-CPA framework, one new code had to be developed. The techincal problems related to the KKR structure constants calculations and the Brillouin Zone integration for an arbitrary Bravais lattice, the two major tasks of the extensions, have been described in ref. [10]. Here we give a very brief list of the features of a new method for the Brillouin Zone integration of KKR-type functions, that have a pole structures, but is easily extensible to any band theory.

The method sets an adaptive grid of lines in the irreducible segment of the Brillouin Zone, and perform the integrals along the lines by means of a local fit by rational functions of the integrand. The integrals in the direction grid is performed by means of and adaptive technique, based on an iterative "local" halving of the integration intervals whenever the relative difference of three points trapezoidal rule and Simpson's rule integrals is greater than an arbitrary input tolerance, ϵ. This method proves particularly efficients for KKR functions, where a precise integral can be obtained by calculating the integrand functions only in a neighbourhood of a pole, and this is precisely what the method does. In ref. [10] we compare the results of this method with others.

However, the most interesting feature of the method is that allows to get Brillouin Zone integrals correct within an error proportional to ϵ. As a consequence one could put error bars in the total energy calculations.

Benefits from the Network:

Computer Codes received:
Magnetocrystalline anisotropy energy and spin polarised relarivistic KKR-CPA codes for cubic lattices from Warwick Group (J.B. Staunton and S.S.A. Razee).

Computer Codes jointly developed(Warwick Group):
Magnetocrystalline anisotropy energy for any Bravais lattice.

Other important benefits:
We are aware that our work has been enriched by the scientific contacts offered by the Network and by the discussions with the members and their coworkers from outside the Networks (e.g. Eastern European countries).

Workshop Organization:
Our group organised Ψ_k Network International Workshop on Parallel Algorithms for Large System, held in Taormina ,26-28 November 1994 which has been supported by Ψ_k Network, Regione Siciliana and Local Funds.

Computer Codes:
Bloch Spectral Function (KKR-CPA) Code for cubic lattices passed to Warwick (J.B. Staunton) and Bristol (B.L.Gyorffy) Groups.
Code for Brillouin Zone integration using the Hybrid Method of E.Bruno and B.Ginatempo passed to Warwick Group (J.B. Staunton).
Spin-polarized relativistic Bloch Spectra Function Code for any Bravais lattices passed to Warwick Group (J.B. Staunton).

References

[1] I.M. Lifshitz, Zh. Eksp. Teor. Fiz., **33**, 1569 (1960) [Sov. Phys. JETP, **11**, 1130 (1960)].

[2] E. Bruno, B. Ginatempo, E.S. Giuliano, A.V. Ruban and Yu.Kh. Vekilov, Phys. Rep., **249**, 353 (1994).

[3] E. Bruno, B. Ginatempo, E.S. Giuliano, Phys. Rev. B **52**, 14544 (1995).

[4] E. Bruno, B. Ginatempo, E.S. Giuliano, Phys. Rev. B **52**, 14557 (1995).

[5] J.S. Faulkner, Y. Wang and G.M. Stocks, Phys Rev. B **52**, 17106 (1995).

[6] I.A. Abrikosov, A.M.N. Niklasson, S.I. Simak, B. Johansson, A.V. Ruban and H.L. Skriver, Phys. Rev. Lett. **76**, 4203, (1996).

[7] B.L. Gyorffy and G.M. Stocks, Phys. Rev. Lett. **50**, 374 (1983).

[8] . B.L. Gyorffy, D.D. Johnson, F.J. Pinski, D.M. Nicholson and G.M. Stocks, in *Alloy Phase Stability*, G.M. Stocks and A. Gonis eds., NATO ASI Series vol. E **163**, p. 421, (Kluwer Academic, Dordrecht, 1989).

[9] E.Bruno and B. Ginatempo, submitted to Phys. Rev. Lett. (1997).

[10] E. Bruno and B. Ginatempo, Phys. Rev. B **55**, 12946 (1997).

Scientific Highlights

The Psi-k network encouraged us right at the start to organize a one-day meeting in Muenster on Green function methods, and scientists came from Germany, Greece and The Netherlands to discuss applications to surface electronic structure, photoemission, and electronic structure in general. Another, smaller meeting was organized in Nijmegen in 1994 to discuss calculations of dielectric functions, when scientists from Dublin, Twente and Nijmegen got together to discuss bond models and electron gas methods for dielectric functions. This meeting has in fact led to the participation of Twente (Wijers) in the Network, and collaboration between Twente and Dublin.

The Network facilitated several very useful trips abroad. In January 1995 Jeroen van Hoof, Martina Heinemann and John Inglesfield visited the group of Podloucky in Wien to discuss embedded LAPW calculations of surfaces versus slab LAPW calculations. We are still in discussion, so this was a useful contact. Jos Thijssen, then Nijmegen but now Cardiff, participated in the network conference on order(N) methods, and this has led to new research activities. Since Inglesfield moved to Cardiff, the network has funded visits to Cardiff of Jeroen van Hoof and Patrick Slavenburg to discuss their research, and of John Inglesfield to Nijmegen. Several papers are being written up in the fields of surfaces, interfaces and alloys as a consequence of these visits. The visits also enabled Jeroen van Hoof to mount his embedded electronic structure codes on the Cardiff machines, and this is proving invaluable for the research activities in Cardiff.

The highlight of Psi-k activities in Nijmegen was the development by Jeroen van Hoof, in collaboration with Simon Crampin (Bath) and Inglesfield, of the new embedding method, which can be used to calculate the electronic structure of surfaces, interfaces and bulk material self-consistently, taking into account the substrate on the same footing as the region being embedded. In this method, the system is divided up into layers which are embedded onto other layers to build up the surface, interface or bulk. The new code has been used to calculate surface and interface electronic structure, and the most exciting applications to date are by Van Hoof in collaboration with workers from Delft and Philips on magneto- resistance through metallic multilayer systems.

The following published papers acknowledge network support:

Embedding method for confined quantum systems,
S. Crampin, M. Nekovee and J.E. Inglesfield,
Phys. Rev. B51 7318 (1995).

Generating tight-binding Hamiltonians with finite-difference methods,
J.M. Thijssen and J.E. Inglesfield,
Phys. Rev. B51 17988 (1995).

Quantum-well states in Cu/Co overlayers and sandwiches,
P. van Gelderen, S. Crampin and J.E. Inglesfield,
Phys. Rev. B53 9115 (1996).

Effect of interface magnetic moments and quantum-well states on magnetization-induced second-harmonic generation,
P. van Gelderen, S. Crampin, Th. Rasing and J.E. Inglesfield,
Phys. Rev. B54 R2343 (1996).

$TiFe_{1-x}Co_x$ alloys and the influence of anti-structural atoms,
P. Slavenburg,
Phys. Rev. B **55**, 16110 (1997).

Scientific Highlights

During the Network period and to a large extent as a consequence of the Network structure, the Aarhus node initiated a collaboration with the Daresbury node and the Karlsruhe node on the application of self-interaction corrected electronic structure calculations to rare earth materials. This has resulted in 2 publications, [1],[2], and two in preparation [3], [4].

Conventional electronic structure methods fail badly in the description of materials characterized by localized f-electrons, while the SIC-LSD method presents a scheme to describe the electrons as either localized or delocalized. In [1] the series of Cerium Pnictides was studied and the experimental trends in structures as a function of hydrostatic pressure reproduced. In particular, for CeP an isostructural rocksalt→rocksalt phase transition is observed at a pressure of 55 kbar with a $\sim 10\%$ volume kollapse. The calculations show this to occur as a consequence of the Ce f-electron changing character from being localized to being delocalized. The calculated transition pressure is 79 kbar. Similar transitions are found in CeAs, CeSb and CeBi, however accompanied by change in crystal structure (to the CsCl structure). In all cases the experimentally observed phase transitions are reproduced, and additional phase transitions are predicted at high compressions (see Table).

Table 2: Calculated and experimental transition pressures for the electronic and structural phase transitions in the cerium pnictides. The errorbars in the quoted experimental transition pressures are estimates based on the hysteresis loop observed in the experimental PV curves. Also quoted are the specific volumes on the two sides of the transition. The notation (d) and (l) refers to calculations with delocalized or localized Ce $f-$electrons, i.e. tetravalent or trivalent Ce atoms. B2* denotes the distorted B2 structure.

compound	transition	P_t (kbar)		V_h ($a_0{}^3$)		V_l ($a_0{}^3$)	
		theo.	expt.	theo.	expt.	theo	expt.
CeN	B1(d) → B2(d)	620	-	148	-	141	-
CeP	B1(l) → B1(d)	71	90,55	325	308	297	298
CeP	B1(d) → B2(d)	113	150(40)	288	285	246	247
CeAs	B1(l) → B2(d)	114	140(20)	332	315	265	274
CeSb	B1(l) → B2*(l)	70	85(25)	400	398	353	354
CeSb	B2*(l) → B2*(d)	252	-	311	-	295	-
CeBi	B1(l) → B2*(l)	88	90(40)	427	399	376	360
CeBi	B2*(l) → B2*(d)	370	-	317	-	304	-

The Ytterbium Pnictides were subsequently studied [4]. Here the heavy fermion character of these compounds were reproduced, and the gradual change from trivalent to divalent Yb behavior

from YbP over YbAs and YbSb to YbBi reproduced.

1. A. Svane, Z. Szotek, W. M. Temmerman and H Winter, *Theory of the Electronic and Magnetic Structure of Cerium Pnictides under Pressure*, Solid State Commun. **102**, 473 (1997).

2. W. M. Temmerman, A. Svane, Z. Szotek and H. Winter, *Applications of Self-Interaction Corrections to Localized States in Solids*, in 'Electronic Density Functional Theory: Recent Progress and New Directions', Eds J. F. Dobson, G. Vignale and M.P. Das (Plenum, 1997.)

3. A. Svane, J. Lægsgaard, Z. Szotek, W. M. Temmerman and H Winter, *Electronic and Magnetic Structure of Cerium Pnictides under Pressure*, 1998, in preparation.

4. W. M. Temmerman, A. Svane, Z. Szotek and H. Winter, *Self-Interaction Corrected Theory of Ytterbium Pnictides*, 1998, in preparation (preliminary results presented at the Schwäbisch Gmünd Conference).

5. J. Lægsgaard and A. Svane, *Three-particle Approximation for Transition Metal Oxides*, Phys. Rev. B**55**, 4138 (1997).

Improved Density Functionals and Reduced (0-1-2) Dimensionality Working Groups

Nodes: **Modena and Trento**

Scientific Highlights

The activity of the Modena and Trento nodes has been devoted to study i) the effects of on-site correlation in narrow band materials, ii) the optoelectronic properties of confined systems, iii) electronic properties of superconductor-semiconductor superlattices.

i) On-site correlation in narrow band materials.

The physics of materials such as transition metals, transition metal oxides, cuprates, etc.. is dominated by the competition between inter-site hopping and on-site electron-electron repulsion. In these systems in fact the itinerant character of valence electrons coexists with strong local correlations responsible of spectroscopical features such as satellites , band-narrowing and opening of Mott-Hubbard gaps. In spite of the enormous amount of theoretical and experimental work which has been done on cuprates since the discovery of high T_c superconductors, an unified theoretical description of the whole valence spectrum, from the high binding energy region, dominated by satellites, up to the valence band top, including both unperturbed single particle like and strongly correlated Cu derived structures, is still missing; this is due to the difficulty to combine an accurate treatment of many body terms with a realistic description of the band structure.

We have developed a method which includes both the hybridization between Cu and the ligands (or between sp and d states in the case of transition metals) accounted for by first principle band theory, and a treatment of e-e interaction which must be non-perturbative - to deal with systems which are in the high correlation regime - and beyond mean field - to include finite lifetime excitations. This approach allows to augment conventional band theory via the inclusion of on-site correlation: the single-particle band states are determined according to the density functional theory in the local density approximation (LDA) and the localized e-e interaction is described as a 3-body scattering (3BS) solution of a multi-orbital Hubbard Hamiltonian.

The 3BS method can be seen as an extension to the solid state of the configuration-interaction scheme used for finite systems (molecules and clusters): the Hubbard Hamiltonian is projected on a set of states obtained by adding a finite number of e-h pairs to the ground state of the single-particle Hamiltonian and this expansion is truncated to include just one e-h pair. The effect of electron correlation on one electron removal energies from a partially filled band is then described as hole-hole and hole-electron interaction. The 3BS theory corresponds to the solution of a 3-body scattering problem involving two holes and one electron.

The method can be applied to the study of both valence and core states. where again the interplay between the localized and itinerant character of electron states is crucial to describe the response of an itinerant electron system to the creation of a core hole, dominated by the

many-body effects associated to the on-site coupling between localized (core) and itinerant (valence) states.

ii) optoelectronic properties of confined systems

The discovery of intense visible room temperature photoluminescence from porous Si has raised a renewed interest in understanding the electronic structures of low dimensional Si nanostructures. In particular, structures microscopically well characterized are desirable for the understanding of luminescence through a comparison between theoretical and experimental results. In particular we have study how the quantum confinement effect modifies the electronic and optical properties of semiconductor systems of low dimensionality:

a) Small Silicon Clusters

We have study the electronic structure and optical activity of small hydrogen-saturated Si clusters, through an approach which can treat both small molecules and bulk crystals. Our scheme fully incorporates the correlation effects that become critical in the small-cluster limit. We find that, when correlation is properly included, even small clusters of ~ 50 Si atoms can be active in the visible range ($h\nu \sim 1.6 - 1.9$ eV). Furthermore this activity is associated with the "crystalline" silicon in the core of the cluster, thus confirming the role of quantum confinement as generating the visible emission.

b) Quantum confined semiconductor slabs

Semiconductor structures microscopically well characterized are desirable for the understanding of luminescence through a comparison between theoretical and experimental results. By performing first principle LMTO calculations of ultra-thin Si(111) layers (1-7 Si double layers (dL)) embedded in CaF_2 we were able to begin correlating the electronic properties of Si nanostructures with their structural properties in a systematic way. We have checked the quantum confinement hypotesis for the Si band opening as a function of thickness and pointed out the different nature of valence and conduction band states in the energy region around the gap. In order to better understand the role of interface states and chemical deposition on the mechanisms of light emission at Si surfaces, we have also studied the different behavior of Ca and H bonds at the Si surface. Using the same theoretical method we have studied the dependence of the electronic properties of Si(111) slabs saturated by hydrogen atoms on the two sides of the slabs. In this way we obtain results for the H-Si-H system, which are directly comparable with the corresponding results for the CaF_2-Si-CaF_2 superlattice. Moreover in order to further investigate the role of the saturating agent we have performed investigation replacing the H atoms on one side of the Si slabs by OH groups. Indeed we have study, even using the LMTO-ASA approach the electronic properties of confine rare earth arsenides in gallium arsenide, showing the possible conditions for a gap opening in the rare earth arsenides compounds.

c) Si quantum wires

The purpose of this task was to show that reliable selfconsistent density of states and energy bands for complicated Si quantum wire systems can be obtained using an electron method (LMTO), which makes possible the calculation of both valence and core states. For these systems we have also developed an extension of our calculations, which enables the computation of the optical matrix elements. This is an important application in order to indagate the nature and

the properties of the light-emitting states in the quantum confined Si wires. The results show the opening of the band gap, their quasi-direct nature and the different role of quantum confinement for valence and conduction band states. Detailed comparison has been made between the theoretical results and the experimental outcomes regarding core level shift, Auger lineshape, luminescence properties. Moreover we have performed combined LMTO and Pseudopotential calculations to elucidate the role of dangling bonds, surface states and chemical deposition and modifications (e.g. formation of H-Si bonds, role of the Si-SiO_2 , Si-Ca and Si-F bonds) on the mechanisms of light emission.

iii) Electronic properties of superconductor-semiconductor superlattices.

One of the central problem in the theory of high-T_c superconductivity is to what extent the superconducting properties are bound to the two dimensionality of the CuO_2 planes, and how the extension into the third dimension is achieved by the coupling between adjacent CuO_2 planes. Charge transfer effects in $YBa_2Cu_3O_7$/ $PrBa_2Cu_3O_7$ superlattices have been proposed by many authors as the origin of the experimentally observed strong depression of the critical temperature. We performed self-consistent LMTO-ASA calculations and found that no remarkable change in the electronic structure of the superconducting CuO_2 planes occurs in the studied structures, when the PBCO layer thickness is varied. The observed depression of the critical temperature does not seem to be originated intrinsically by a severe modification of the electronic structure or by the hole-filling mechanism.

Electronic Structure in the Normal and in the Superconducting State Working Group

Nodes: **Bristol-Daresbury-Stuttgart-Würzburg**

Electronic structure in the normal and superconducting states.

Balazs L. Gyorffy (convener of the Working Group)
University of Bristol, UK

The four nodes involved in this Working Group are: Daresbury Laboratory (*Z. Szotek and W.M. Temmerman*), University of Bristol (*B.L. Gyorffy, P. Miller, and J.F. Annett*), Max-Planck-Institute in Stuttgart (*O.K. Andersen and O. Jepsen*), and University of Würzburg (*E.K.U. Gross, K. Capelle, M. Lüders, and S. Kurth*). The activities during the review period were driven by needs of close and very fruitful scientific collaboration which resulted in a number of significant papers (see below). They took the form of research visits and weekend workshops and, in addition to refereed publications, they were reported on, regularly, in the HCM Ψ_k-Network Newsletter.

The scientific aim of the Group was to adopt the computational techniques for studying the electronic structure of normal metals for the analogous task focused on superconductors. The fact that an enormous amount of expertise is available, particularly within the HCM Ψ_k-Network, about how to calculate the electronic structure of condensed matter from first principles, but none of this has been brought to bear on the description of the superconducting state, lends much impetus to this project. Indeed, we found that the very first implementations of our strategy yielded surprising new insights into the physics of quasi-particles in the superconducting state. Three of the most striking ones of these are highlighted below.

- We found [1, 2, 3] that a relatively simple 8-band model representation of the first-principles, Local Density Approximation (LDA), calculations of the electronic structure of YBCO bilayer gave a very good quantitative account of the superconducting transition temperature T_c, the quasi-particle spectra (see Figure) and the specific heat with only one adjustable parameter. Moreover, these calculations strongly suggest that the effective electron-electron attraction in this high temperature superconductor (HTS) operates between electrons, with anti-parallel spins, on nearest neighbour sites in Cu $d_{x^2-y^2}$ orbitals.
- One of the interesting, generic features of the first-principles calculations of the electronic structure of the HTS matrials, seems to be a set of bifurcated saddle points near the Fermi energy, ε_F. We discovered [4] that the evolution of the relative position of ε_F, with respect to this Van Hove singularity, with doping can give a good quantitative account of the experimentally observed rise and fall of T_c accompanying such changes. Such evidence in

support of the Van Hove scenario may turn out to be a significant step towards solving the central problem of HTS, namely identifying the mechanism of pairing.

- We formulated a relativistic version of the theory of superconductivity and found, for the first time, the complete form of the spin-orbit interaction as it enters the fundamental, Bogoliubov-de Gennes, equations of superconductivity. A surprising feature of the new theory is dichroism in the absorption of electromagnetic radiation by superconductors. Our predictions [5, 6] are currently attracting considerable experimental interest.

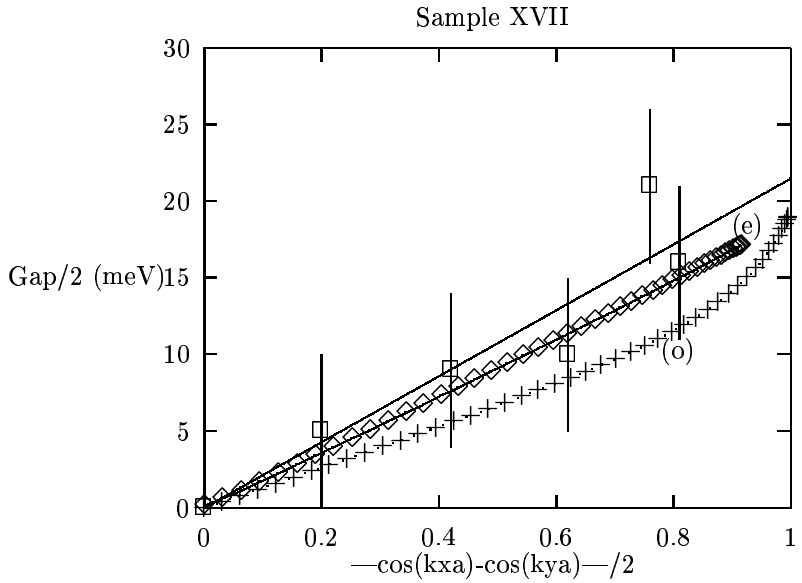

Figure 5: A comparison of the calculated gap for the intra-layer nearest neighbour Cu $d_{x^2-Y^2}$–Cu $d_{x^2-Y^2}$ interaction, for the even (e) and odd (o) sheets of the YBCO Fermi surface, with the experimental data deduced by Schabel et al. (Phys. Rev. B**55**, 2796 (1997)).

References

[1] M.B. Suvasini et al., Phys. Rev. B**48**, 1202 (1993).

[2] W.M. Temmerman et al., Phys. Rev. Lett. **76**, 307 (1996).

[3] B.L. Gyorffy et al., Phys. Rev. B, submitted 1997.

[4] Z. Szotek et al., submitted 1997.

[5] K. Capelle et al., Phys. Rev. Lett. **78**, 3753 (1997).

[6] K. Capelle, Phys. Rev. B, to be published (1998).

Scientific Highlights

Magnetic impurities in simple metals

The presence or absence of a magnetic moment of an impurity diluted in a nonmagnetic metal host is determined by a competition between intra-atomic exchange interaction and interatomic electron motion. Within the framework of the Anderson model, the impurities are distinguished as magnetic and nonmagnetic according to the ratio of two parameters: the mean intra-atomic Stoner exchange energy and the width of the impurity virtual bound state.

The experimental investigations of the magnetic properties of impurities diluted in simple metals were for many years restricted to $3d$ impurities in noble metals and aluminium. Recently, the variety of host materials was extended to include alkali and alkali-earth metals. The relevant experimental studies apply the time-differential perturbed γ-ray distribution method to investigate the local magnetic behaviour of impurities implanted by recoil into the host crystal. Alkali and alkali-earth metals provide a wide range of host free-electron densities ρ, and thus one can closely study the transition of the impurities from itinerant to atomic configurations.

In collaboration with the Jülich group (P. H. Dederichs and R. Zeller) we have studied extensively the magnetic behaviour of impurities in simple metals by means of first-principles local-spin-density-functional electronic-structure calculations, using both the KKR Green function method and the jellium model. We found that, in the vicinity of the transition from a spin-polarized to a non-spin-polarized impurity state the local moment varies proportionally to $\sqrt{1-\rho/\rho_c}$ for $\rho < \rho_c$. This expression is very similar to the result of the Landau theory for second-order phase transitions and, as it turns out, it also applies to free-electron densities away from the critical point ρ_c [1, 2]. We also predicted that, besides the $3d$ and $4d$ impurities, also the $5d$ and some *sp* impurities are magnetic in the late alkali metals [3].

This project continued also within the framework of the Ψ_k-Network. For this purpose, several visits took place: N. Stefanou and N. Papanikolaou visited Jülich and P. H. Dederichs visited Athens. We have studied the local magnetic properties of impurities at interstitial positions [4], the problem of orbital polarization within the framework of the local-spin-density $+U$ approximation [5], as well as magnetic impurities in alkali-earth metals [6].

Transport properties of aluminium-based dilute alloys

Transport properties, like the Hall coefficient, the magnetoresistance, the thermopower, etc., of dilute metallic alloys at low temperatures are valuable tools in the investigation of both the topography of the Fermi surface of the host crystal and the scattering properties of the impurity atoms.

Detailed and systematic measurements of the galvanomagnetic coefficients (the magnetoresistivity tensor) in a series of aluminium-based dilute alloys, performed at the Research Centre "Democritos" in Athens, showed important variations of these quantities with different solute atoms. These variations are due to the scattering of the electronic states of the anisotropic parts of the host Fermi surface from the impurity potential and have defied so far a consistent interpretation. Although aluminium is a simple metal with a roughly spherical Fermi surface, there are important deviations from the spherical shape with abrupt curvature variations near the Brillouin-zone boundaries. The fact that the detailed structure of these strongly anisotropic regions plays the most decisive role in the determination of the low-field galvanomagnetic coefficients makes the calculation of these quantities cumbersome.

In a series of papers we reported a systematic study of the low-temperature thermopower [7] and galvanomagnetic properties at weak fields [8, 9] of aluminium-based dilute alloys with $3d$ and $4sp$ impurities. Our theoretical method relies on the so-called on-Fermi-sphere approximation, which allows us to combine the exact topography of the host Fermi surface, described by the 4OPW model, with the scattering phase shifts, obtained from self-consistent local-density-functional impurity-in-jellium calculations. This method involves an all-electron description of the impurity, which enables us to reliably represent also the case of deep d potentials of the $3d$ impurity series for which an OPW description is not suitable. Thus, weak sp- as well as strong d-resonance scattering are treated on the same footing. The transport coefficients are calculated within the framework of Boltzmann transport theory. The appropriate linearized Boltzmann equation is solved exactly by iteration. For the calculation of the magnetoresistivity tensor, we use an efficient scheme based on a Jones-Zener-like expansion at weak magnetic fields, which leads to a hierarchy of integro-differential equations, that we solve self-consistently by an iterative procedure. Our calculations explain successfully the experimental results.

Lattice relaxations around impurities in metals

A point defect in a crystal, such as a vacancy or an impurity atom, does not only break the periodicity of the one-electron potential, but also induces a displacement of its neighbouring atoms from their ideal lattice positions. These displacements are in fact long ranged, varying with the inverse of the square of the distance from the impurity, and lead to a macroscopic volume change of the crystal. A complete information about this displacement field can be obtained by diffuse X-ray or neutron-scattering experiments but, unfortunatelly, very few systems have been measured. Detailed information about many more systems has been obtained by extended X-ray-absorption fine-structure (EXAFS) measurements, which yield reliable data for the first-nearest-neighbour shifts. In addition, lattice-parameter measurements are available for many systems, giving direct information about the volume changes induced by the impurities.

From the theoretical point of view, the treatment of structural relaxation due to defects in crystals is a difficult task. In the past this problem has been mostly dealt with on a phenomenological basis, e.g. by applying models of lattice statics or continuum theory. A reliable microscopic description of lattice-relaxation effects based on first-principles electronic-structure calculations requires very accurate total energies or forces and has mostly been attempted so far for simple metals and semiconductors on the basis of pseudopotential treatments.

In collaboration with the Jülich group (P. H. Dederichs and R. Zeller), we have extended the full-potential KKR Green function method to treat the structural distortion around impurities in crystals [10]. This is an all-electron method which can be applied also to the case of transition metals where pseudopotential treatments are not appropriate. We applied this method to predict the atomic positions in the neighbourhood of d and sp substitutional impurities in Cu [10, 11] and Al [12], by using both the total energy and the ionic Hellmann-Feynman force methods. We also studied the influence of the lattice relaxation on the magnetic properties of the impurities in these systems. The calculated atomic displacements, total volume changes and local magnetic moments are in good agreement with the experimental data. In addition, our results for the magnetic properties of the $3d$ impurities in aluminium seem to resolve the discrepancy between experiment and previous calculations. For an account of this work, which shows also the efficiency of the method to determine the phonon dispersion curves from a single self-consistent calculation of the coupling constants in real space, we refer to the highlight of the October '97 issue of the Network Newsletter.

For this project, N. Stefanou visited Jülich for one month (September 1996). Also, N. Papanikolaou visited Jülich several times as a Ph.D. student and also worked in Jülich as a postdoc from March to December 1996.

Hyperfine interactions of impurities and adatoms at surfaces

Due to modern electronic-structure calculations, most of the basic processes and properties in simple solid materials are rather well understood. However, this is clearly not true for complex systems with reduced symmetry like, e.g., point defects at surfaces, interfaces, layered structures, etc.. Such complex systems, whether they exist naturally or are artificially fabricated, exhibit a rich variety of interesting physical properties and became in the recent years a subject of considerable interest for fundamental as well as for applied research.

The aim of this project is to study the properties of single adatoms and small clusters at surfaces (and interfaces) with the help of first-principles electronic-structure calculations. Mostly due to the development of scanning tunnelling microscopy (STM), such nanostructures at surfaces have recently received a strongly increasing attention. Compared to the STM techniques, a unique and complementary microscopic information can be obtained from the hyperfine structure of these systems, which is caused by the interaction of the electronic degrees of freedom and the nuclear fields, and became available from experiment in recent years. However, a detailed understanding of the local environment that causes the observed hyperfine structure can only be achieved with the help of *ab-initio* electronic-structure calculations.

During the last decades numerous measurements of magnetic hyperfine fields at impurities and neighbouring host atoms have been performed in bulk ferromagnetic or non-magnetic materials and first-principles theoretical calculations provided a consistent interpretation of the experimental data. However, considerable deviations from the bulk properties might occur when the impurities are located close to or at the surface or an interface. To date, quite a few experiments have been performed with probe atoms positioned in atomic layers close to or at a surface or an interface. This field has been pioneered by the Kostanz group with ^{111}Cd- perturbed-angular-correlation (PAC) experiments on the surfaces of Cu and Ni [13, 14]. While in the past most

experiments had been performed with ^{57}Fe or ^{111}Cd probe atoms, the availability of the ISOLDE facility at CERN makes experiments with new isotopes like Cl, Br, Se or Pd/Rh possible. For instance, Granzer *et al.* [15] from the Hahn-Meitner Institute on Berlin have recently performed interesting experiments for the hyperfine fields of Se adatoms on Ni(111) and Ni(001) surfaces which were found to deviate drastically from the known bulk values. The observed strong deviation of the surface values from the bulk field yields a significant reason for a theoretical treatment of this problem. While the theory in the past focused strongly on magnetism of surfaces and thin films, recently also the magnetic properties of single adsorbate atoms and small clusters received considerable attention [16, 17]. The study of hyperfine interactions in these systems will contribute further to the understanding of electronic structure and magnetism at complex surfaces.

The Jülich group (P. H. Dederichs and coworkers) has developed a KKR Green function program for the calculation of the electronic structure of ideal surfaces, interfaces and layered structures. Also a Green function computer code, based on the atomic-sphere approximation for the potential but using the full multipole expansion for the charge density for point defects at these interfaces is available. In collaboration with the Jülich group we have calculated the electronic structure and the hyperfine fields for all the $3d$ and $4sp$ elements considered as impurities and adatoms at Ni(001) and Fe(001) surfaces. For this purpose, Ph. Mavropoulos visited Jülich from 15 June to 31 August 1997 and worked intensively in close collaboration with the group of Prof. P. H. Dederichs on this project. We are at present analysing our results, which seem to explain successfully the observed drastic reduction of the hyperfine field on Se adatoms on Ni surfaces. As a subsequent step, we plan to implement the full-potential and lattice-relaxation treatments into the computer codes and study their influence on the results.

References

[1] N. Stefanou and N. Papanikolaou, J. Phys.: Condens. Matter **5**, 5663 (1993)

[2] P. H. Dederichs, P. Lang, K. Willenborg, R. Zeller, N. Papanikolaou, and N. Stefanou, Hyp. Int. **78**, 341 (1993)

[3] N. Papanikolaou, N. Stefanou, R. Zeller, and P. H. Dederichs, Phys. Rev. Lett. **71**, 629 (1993)

[4] N. Stefanou, N. Papanikolaou, R. Zeller, and P. H. Dederichs, Physica Scripta **50** 445 (1994)

[5] N. Stefanou, J. Phys.: Condens. Matter **6**, 11221 (1994)

[6] N. Papanikolaou, N. Stefanou, R. Zeller, and P. H. Dederichs, Phys. Rev. B **51**, 11473 (1995)

[7] Ph. Mavropoulos, N. Papanikolaou, and N. Stefanou, J. Phys.: Condens. Matter **7**, 4665 (1995)

[8] N. Papanikolaou, N. Stefanou, and C. Papastaikoudis, Phys. Rev. B **49**, 16117 (1994)

[9] Ph. Mavropoulos and N. Stefanou, J. Phys.: Condens. Matter **9**, 8997 (1997)

[10] N. Papanikolaou, R. Zeller, P. H. Dederichs, and N. Stefanou, Phys. Rev. B **55**, 11473 (1997)

[11] N. Papanikolaou, N. Stefanou, R. Zeller, and P. H. Dederichs, *Stability of Materials*, A. Gonis, P. E. A. Turchi, and J. Kudrnovsky, eds. (Plenum Press, New York, 1996), p.419

[12] N. Papanikolaou, R. Zeller, P. H. Dederichs, and N. Stefanou, Comput. Mat. Sci. **8**, 131 (1997)

[13] J. Voigt, R. Fink, G. Krausch, B. Luckscheiter, R. Platzer, U. Wöhrmann, X. L. Ding, and G. Schatz, Phys. Rev. Lett. **64**, 2202 (1990)

[14] T. Klas, J. Voigt, W. Keppner, R. Wesche, and G. Schatz, Phys. Rev. Lett. **57**, 1068 (1986)

[15] H. Granzer, H. H. Bertschat, H. Haas, W. D. Zeitz, J. Lohmüller, and G. Schatz, Phys. Rev. Lett., **77**, 4261 (1996)

[16] K. Wildberger, V. S. Stepanyuk, P. Lang, R. Zeller, and P. H. Dederichs, Phys. Rev. Lett **75**, 509 (1995)

[17] V. S. Stepanyuk, W. Hergert, K. Wildberger, R. Zeller, and P. H. Dederichs, Phys. Rev. B **53**, 2121 (1996)

Scientific Highlights

In the Vienna node of P. Weinberger at the Center for Computational Materials Science & Institut für Technische Elektrochemie, Technical University of Vienna essentially four rather interrelated topics were dealt with in strong collaboration with non-Austrian members[2] of the HCM network. All four topics were related to problems of semi-infinite systems (solid systems with surface or with interfaces). In particular since magnetic properties of such systems are of enormous technological interest.

Interface exchange coupling

In this particular field of research, various studies were performed such as the effect of alloying the spacer material, of changing the type of magnetic slabs and also the kind of new features to be expected when terminating the multilayer system by a non-magnetic cap. Typical examples of collaborations in this field of research are listed below:

J. Kudrnovský, V. Drchal, P. Bruno, I. Turek and P. Weinberger, *"Interlayer magnetic coupling: effect of alloying in the spacer",* Phys. Rev. B54, R3738 (1996).

J. Kudrnovský, V. Drchal, R. Coehoorn, M. Šob and P. Weinberger, *"Calculated phases of the oscillatory exchange coupling between Fe-Co-Ni alloys across a Cu spacer",* Phys. Rev. Lett. **78**, 358 (1997).

J. Kudrnovský, V. Drchal, P. Bruno, R. Coehoorn, J.J. De Vries, K. Wildberger, P.H. Dederichs and P. Weinberger, *"Effect of cap-layers on interlayer exchange coupling",* MRS Symposium Proceedings (Eds.: J. Tobin et al.) Vol. **475**, 575 (1997).

J. Kudrnovský, V. Drchal, P. Bruno, I. Turek and P. Weinberger, *"Interlayer exchange coupling: effect of the cap-layers",* Phys.Rev. B**56**, 8919 (1997).

Magnetic anisotropy of layered systems

By using a (fully)-relativistic spin-polarized approach quite a few new features of the magnetic anisotropy in magnetic multilayers were found such as oscillations in the interface exchange coupling, anomalous enhancement when considering a cap of non-magnetic material, but also

[2]Non-Austrian coauthors from the HCM network are underlined.

oscillatory behavior of the magnetic anisotropy energy. It was even shown that for certain systems an ab-initio determination of anisotropy constants is possible. Again below are examples of such research as an outcome of collaboration with non-Austrian members of the HCM network.

L. Szunyogh, B. Úfalussy, P. Weinberger and C. Sommers, *"Fully relativistic spin-polarized description of interface exchange coupling for Fe multilayers in Au(100)",* Phys.Rev. **B54**, 6430 (1996).

B. Úfalussy, L. Szunyogh, P. Bruno and P. Weinberger, *"First principles calculations of the anomalous perpendicular anisotropy of a Co monolayers on Au(111)",* Phys. Rev. Lett. **77**, 1805 (1996).

P. Weinberger, C. Sommers, U. Pustogowa, L. Szunyogh and B. Újfalussy, *"Ab-initio determination of magnetic interface coupling constants",* J. Phys. I France **7**, 1299 (1997).

L. Szunyogh, B. Úfalussy, C. Blaas, U. Pustogowa, C. Sommers and P. Weinberger, *"Oscillatory behavior of the magnetic anisotropy energy in Cu(100)/Co_n multilayer systems",* Phys.Rev.B**56**, 14 036 (1997).

Screened KKR & transport for multilayer systems

Since it is also always necessary to improve the theoretical tools to be used in numerical applications, some research was devoted to a generalization of screening with a multiple scattering approach, but also to the use of such an approach in order to calculate transport properties:

R. Zeller, P.H. Dederichs, B. Úfalussy, L. Szunyogh and P. Weinberger, *"Theory and convergence properties of the Screened Korringa-Kohn-Rostoker method",* Phys.Rev.**B52**, 8807 (1995).

P. Weinberger, P.M. Levy, J. Banhart, L. Szunyogh and B. Úfalussy, *"Band structure and electrical conductivity of disordered semi-infinite systems",* J.Phys.Cond.Matt. **8**, 7677 (1996).

Alloy theory

As part of the studies devoted to non-magnetic systems order phenomena of two-dimensional alloys at the surface were investigated and in particular great attention was given to a careful discussion of an Ising-type description of surface segregation. As can be seen from the list below, also here the interaction with the HCM network proofed to be extremely useful.

R. Tetot, J. Kudrnovský, A. Pasturel, V. Drchal and P. Weinberger, *"Phase diagram of the Cu-Pd surface alloy",* Phys. Rev. **B51**, 17 910 (1995).

V. Drchal, J. Kudrnovský, A. Pasturel, I. Turek and P. Weinberger, *"Ab-initio theory of surface segregation: selfconsistent determination of the concentration profile"*, Phys. Rev. **B54**, 8202 (1996).

Application of current density functional theory to spontaneously magnetised solids

H. Ebert, Marco Battocletti, and T. Huhne
Institute for Physical Chemistry, University of Munich,
Theresienstr. 37, D-80333 München, Germany
and
E.K.U. Gross
Institute for Theoretical Physics, University of Würzburg,
Am Hubland, D-97074 Würzburg

Recently there has been a lot of interest in properties of magnetic solids that are caused by spin-orbit coupling. Some few examples for these are the magneto-crystalline anisotropy [1], galvano-magnetic effects [2] and various dichroic phenomena in electron spectroscopy [3]. Corresponding theoretical investigations are in general performed within the framework of local spin density functional theory (SDFT). The influence of spin-orbit coupling is accounted for either in the variational step of a conventional $\vec{k}$-space band structure method [4] or by working on the basis of the Dirac equation for a spin dependent potential.[5, 6]

The most prominent shortcoming of this approach is that it gives the spin-orbit induced orbital magnetic moment of transition metals up to 60% too small compared to experiment. The main reason for this is that local SDFT is primarily coined to account for spin polarization and therefore supplies even in its present proper relativistic form [7, 8] an insufficient theoretical basis to calculate quantities connected with the orbital electronic current [9]. To overcome this problem Brooks and coworkers [10, 11] introduced the so-called orbital polarization (OP) formalism, that was borrowed from atomic theory and is meant to account for Hund's second rule i.e. to maximize the orbital angular momentum.

In contrast to the OP-formalism, the current density functional theory (CDFT) has a firm basis, does not leave the framework of density functional formalism and should also cure or reduce the above mentioned problems. Starting from a relativistic formulation based on quantum electrodynamics such an approach has been worked out first by Rajagopal and Callaway [12]. The resulting Dirac-Kohn-Sham equation for a system without external vector potential reads as follows

$$\left[c\vec{\alpha}\cdot\left(\frac{\hbar}{i}\vec{\nabla}+\frac{e}{c}\vec{A}_{xc}\right)+\beta mc^2+V_H(\vec{r})+V_{xc}(\vec{r})\right]\Psi_i(\vec{r})=\epsilon_i\Psi_i(\vec{r})\ . \tag{5}$$

Here the exchange-correlation scalar and vector potentials V_{xc} and $\vec{A}_{xc}$, respectively, are functionals of the density n and the physical (gauge-invariant) current density $\vec{j}$. Unfortunately no parametrisation for the corresponding exchange-correlation energy is available so far. Vignale

and Rasolt [13, 14, 15], on the other hand, derived a consistent non-relativistic formulation of CDFT in terms of the paramagnetic current density $\vec{j}_p$ and suggested an appropriate parametrisation for the exchange-correlation energy.

The Vignale–Rasolt CDFT-formalism can be obtained as the weakly relativistic limit of Eq. (5). This property has been exploited to set up a computational scheme that works in the framework of CDFT and accounts for the spin-orbit coupling at the same time. In practice this means that a hybrid scheme has been developed where only the kinematic part of the problem is dealt with in a fully relativistic way whereas the exchange-correlation potential terms are treated consistently to first order in $1/c$. The corresponding modified Dirac equation that automatically accounts for the spin-orbit coupling and at the same time incorporates a term that explicitely represents a coupling to the electronic orbital degree of freedom is given by:

$$\left[-i\hbar c\vec{\alpha}\cdot\vec{\nabla}+\beta mc^2+V_{eff}(\vec{r})+\beta\sigma_z\cdot B_{eff}(\vec{r})+\sum_\sigma \beta H_{op,\sigma}P_\sigma\right]\Psi_i(\vec{r})=\epsilon_i\Psi_i(\vec{r})\,. \tag{6}$$

As within standard SDFT the scalar potential terms V_{eff} and B_{eff} stand for the average and difference, respectively, of the two spin-dependent potentials $V_H + V_{xc,\sigma}$. The additional term with

$$H_{op,\sigma}=-\frac{i\hbar e}{2mc}\left[\vec{A}_{xc,\sigma}(\vec{r}),\vec{\nabla}\right]_+ \tag{7}$$

represents the coupling of the orbital current and the exchange-correlation vector potential $\vec{A}_{xc,\sigma}$. Since in the present formalism $\vec{A}_{xc,\sigma}$ is defined in a spin-dependent way, the spin-projection operator $P_\sigma = \frac{1\pm\beta\sigma_z}{2}$ appears, in addition to $H_{op,\sigma}$, in Eq. (6).

The scheme sketched above has been implemented by applying appropriate extensions to a spin polarized relativistic Korringa-Kohn-Rostoker-Green's function (SPR-KKR-GF) band structure program working in the atomic sphere approximation (ASA) as well as to corresponding routines for the core states. Within the Wigner-Seitz sphere the particle density n_σ was taken to be spherically symmetric. The current density $\vec{j}_{p,\sigma}$, on the other hand, was taken to be rotationally symmetric with the symmetry axis pointing along the direction of the magnetisation, which in turn was fixed parallel to the crystallographic z-axis. This means that $\vec{j}_{p,\sigma}$ is everywhere parallel to the polar unit vector $\vec{e}_\phi$ and depends only on the spherical coordinates r and θ. For that reason the resulting exchange-correlation vector potential $\vec{A}_{xc,\sigma}$ is also parallel to $\vec{e}_\phi$ and rotationally symmetric. This has the important consequence that the coupling term in Eq. (7) causes no further reduction in symmetry compared to a conventional spin polarized relativistic calculation based on SDFT. An analysis of the results for $\vec{A}_{xc}$ shows that it depends only weakly on the azimuthal angle θ. For that reason the average of $\vec{A}_{xc}$ with respect to θ has been used to simplify the solution of the radial Dirac equations.

Obviously one of the central quantities of CDFT is the paramagnetic current density $\vec{j}_{p,\sigma}$. For bcc-Fe the valence band part of $\vec{j}_{p,\sigma}$ obtained with our approach is shown in Fig. 6. When suppressing any potential term in the Dirac equation that couples to the orbital current, the spin-orbit induced current density $\vec{j}_{p,\sigma}$ scarcely depends on whether the calculations are performed in the ASA-mode or a full potential (FP) mode (FP-OP-SPR-KKR). In fact the spin-resolved results shown in Fig. 6 have been obtained from full potential SPR-KKR calculations [17]. An angular momentum decomposition of $\vec{j}_{p,\sigma}$ reveals that – as one expects – it is nearly exclusively due to the d-electrons. Accordingly, its radial distribution is closely linked to the corresponding

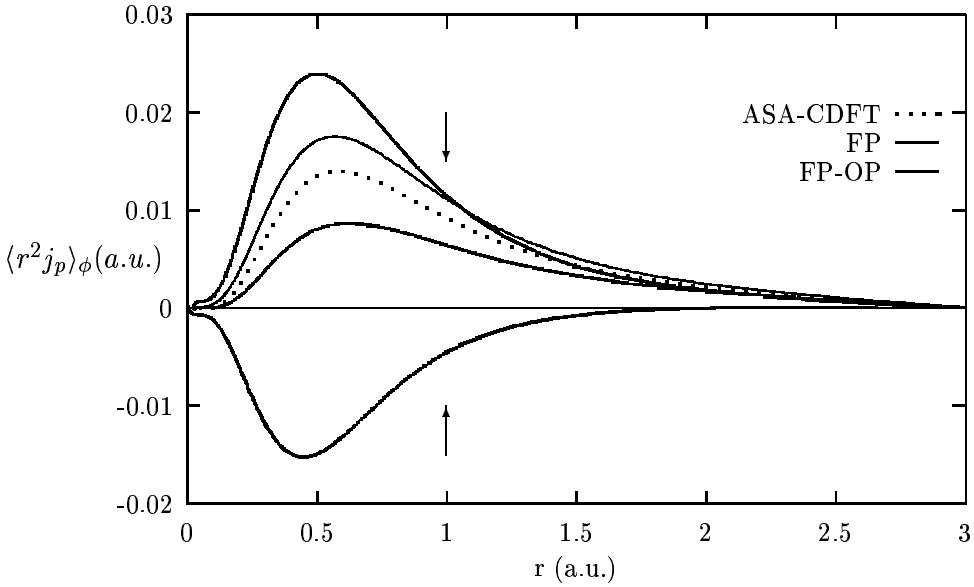

Figure 6: Magnitude of $r^2\vec{j}_p$ for bcc-Fe in the (100)-plane ($\theta = \frac{\pi}{2}$) and averaged with respect to its ϕ-dependence. The various curves show results stemming from FP-SPR-KKR (FP) calculations based on the plain SDFT-Dirac equation, calculations including the OP-term (FP-OP) and work done within CDFT using the ASA-SPR-KKR (ASA-CDFT) [16], respectively. In addition the decomposition of the FP-result into its spin-projected contributions $\vec{j}_{p,\uparrow(\downarrow)}$ is given marked with arrows $(\uparrow, \downarrow)$.

radial wave functions. As can be seen both spin-parts $\vec{j}_{p,\sigma}$ are of opposite sign and differ in a pronounced way in magnitude. Connected with $\vec{j}_{p,\sigma}$ there are corresponding orbital angular momenta $\langle l_z \rangle_\sigma$ that in turn give rise to the orbital magnetic moment $\mu_{orb} \approx \mu_B \sum_\sigma \langle l_z \rangle_\sigma$ which is obviously dominated by its minority spin contribution [18]. There is a rather appreciable contribution to $\vec{j}_{p,\sigma}$ due to the core electrons. However, the contributions for different spin character nearly cancel each other and for that reason these have not been included in Fig. 6.

The valence band contribution to the exchange-correlation vector potential $\vec{A}_{xc,\sigma}$ obtained for bcc-Fe within CDFT is shown in Fig. 7 for $\theta = \pi/2$. Obviously, $\vec{A}_{xc,\sigma}$ is much larger for the minority than for the majority spin direction as it was found for the current density distribution. However, the vector potential possesses a rather complex radial variation that shows no direct and simple relationship to the corresponding current density $\vec{j}_{p,\sigma}$. Again, as for $\vec{j}_{p,\sigma}$, there are quite appreciable contributions to $\vec{A}_{xc,\sigma}$ from the core states in the region near the nucleus. However, suppression of these contributions has hardly any influence on the orbital magnetic moment μ_{orb}. For that reason one can conclude that the variation of $\vec{A}_{xc,\sigma}$ in the region between $r \approx 1$ a.u. (Bohr radius) and the Wigner-Seitz-radius is most important for μ_{orb}.

Application of the SPR-KKR method in the framework of relativistic SDFT leads to 2.27, 1.57 and 0.57 μ_B for the spin magnetic moments of bcc-Fe, fcc-Co and fcc-Ni, respectively. These values agree within a few percent with experiment and change by less than 1% when the the CDFT-formalism is adopted. As Fig. 8 shows, quite pronounced deviations from experiment occur if the orbital magnetic moment μ_{orb} is calculated using the plain SPR-KKR. This discrepancy is reduced for the CDFT-formalism which obviously has the effect of enhancing the spin-orbit induced orbital moments. However this enhancement is somewhat too small for Fe,

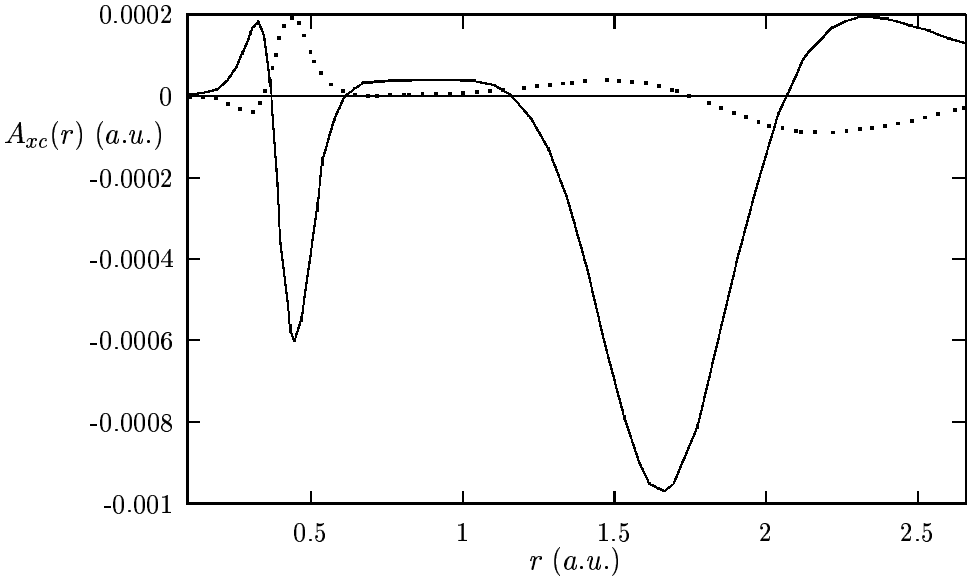

Figure 7: Valence band part of the polar component of the spin-dependent exchange-correlation vector potential $\vec{A}_{xc,\sigma}(r,\theta)$ for bcc-Fe (in atomic units). The full and dashed lines give the potential for minority and majority character, respectively, for $\theta = \pi/2$.

while it is much too small for Co. There are several possible reasons for this: First of all one has to note that the parametrisation used for the CDFT exchange-correlation energy based on linear response theory has only a certain range of applicability which is definitively left for the systems investigated here. In addition one may expect that the various technical approximations made to implement the CDFT have their influence on the final result, making a full potential treatment necessary. Nevertheless, these first results obtained for magnetic solids using the CDFT are encouraging and it can be expected that the observed deviation from the experimental values will be reduced with better parametrisations available [21].

By taking the average of $\vec{A}_{xc,\sigma}$ with respect to the angle θ, the term $-\frac{i\hbar e}{2mc}\left[\vec{A}_{xc,\sigma}(\vec{r}),\vec{\nabla}\right]_+$ in Eq. (7) may be replaced by $\frac{e}{2mc}\frac{\overline{A}_{xc,\sigma}}{r\sin\theta}\hat{l}_z$ where $\hat{l}_z$ denotes the z-component of the orbital angular momentum operator. This term is similar in form to the expression $B_\sigma^{OP}(r)\hat{l}_z$ recently obtained within the extended orbital-polarization (OP) formalism [20] that introduces a potential term instead of using just an energy shift as proposed originally by Brooks [10]. Obviously, B_σ^{OP} can be seen as a vector potential coupled to the orbital current represented by $\hat{l}_z$. However, one has to keep in mind that the physical picture behind the OP-formalism is quite different from the CDFT as used here. While for the former case one tries to account in an approximate way for intra-atomic correlations the vector potential occurring within CDFT is due to diamagnetic contributions to the exchange-correlation energy of the electron gas. Accordingly it is not surprising that the resulting vector potential function (see Fig. 9) for the OP-formalism is quite different from that obtained within CDFT. In spite of this fundamental difference one finds the current density $\vec{j}_{p,\sigma}$ calculated within the extended OP-formalism to be very similar to that calculated within the framework of CDFT. The corresponding curves shown in Fig. 6 differ only in their absolute magnitude (this applies for $\vec{j}_{p,\sigma}$ as well as $\vec{j}_p$) with the total current density $\vec{j}_p$ of bcc-Fe being higher compared to the CDFT-result when calculated with the OP-formalism. As a consequence the deviation from experiment for the corresponding orbital magnetic moment

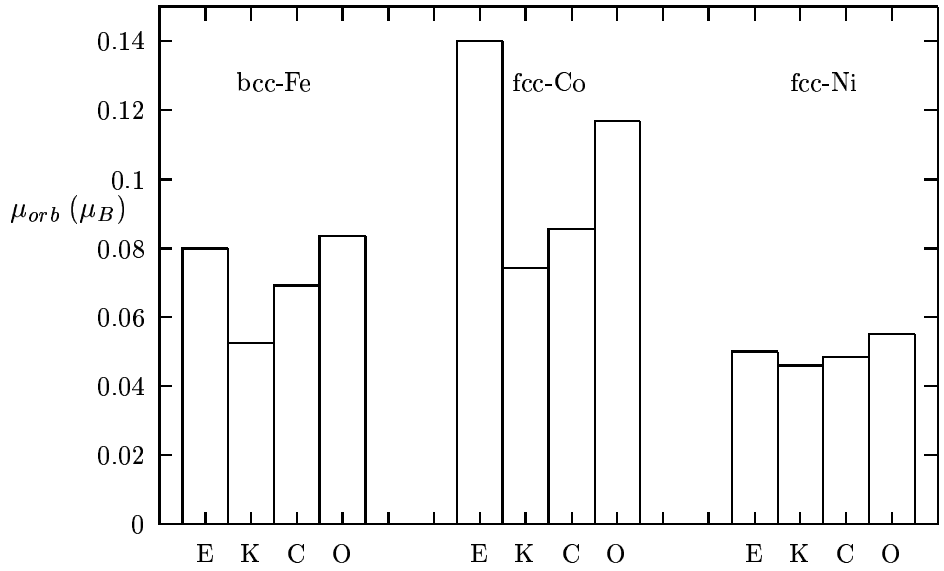

Figure 8: Orbital magnetic moments for bcc-Fe, fcc-Co and fcc-Ni. The columns denoted by E, K, C, and O represent from left to right the experimental data [19] and the theoretical data obtained by the plain SPR-KKR-, within CDFT as described in the text as well as the OP-SPR-KKR [20] including the OP-potential term.

is reduced for Fe and also for Co (see Fig. 8). From these results one may conclude that the OP-formalism, that is extremely simple to be implemented, may be used to study the influence of corrections to the exchange-correlation energy due to finite orbital currents as long as no better parametrisations for this have been derived within CDFT.

Finally, it seems worth to address a special feature of the non-relativistic CDFT Kohn-Sham equation. This equation differs from the ordinary SDFT Kohn-Sham equation by the appearance of the exchange-correlation vector potential $\vec{A}_{xc}$. This term ensures that the single-particle orbitals resulting from the CDFT equations not only reproduce the spin densities n_σ but also the current densities $\vec{j}_{p,\sigma}$ of the interacting system of interest. Since the exchange-correlation potential breaks time reversal symmetry it is conceivable that non-relativistic CDFT without additional spin-orbit coupling might lead to a finite orbital magnetic moment. To investigate this question we performed a calculation including spin-orbit coupling that led to a finite orbital magnetic moment. Then, starting with this solution, the spin-orbit coupling was switched off [22]. In the subsequent self-consistent iterations the orbital magnetic moment approached zero, demonstrating that the presence of $\vec{A}_{xc}$ alone cannot sustain a finite orbital magnetic moment.

References

[1] B. Újfalussy, L. Szunyogh, P. Bruno, and P. Weinberger, Phys. Rev. Letters **77**, 1805 (1996).

[2] J. Banhart and H. Ebert, Europhys. Lett. **32**, 517 (1995).

[3] *Spin-orbit influenced spectroscopies of magnetic solids*, Vol. 466 of *Lecture Notes in Physics*, edited by H. Ebert and G. Schütz (Springer-Verlag, Heidelberg, 1996).

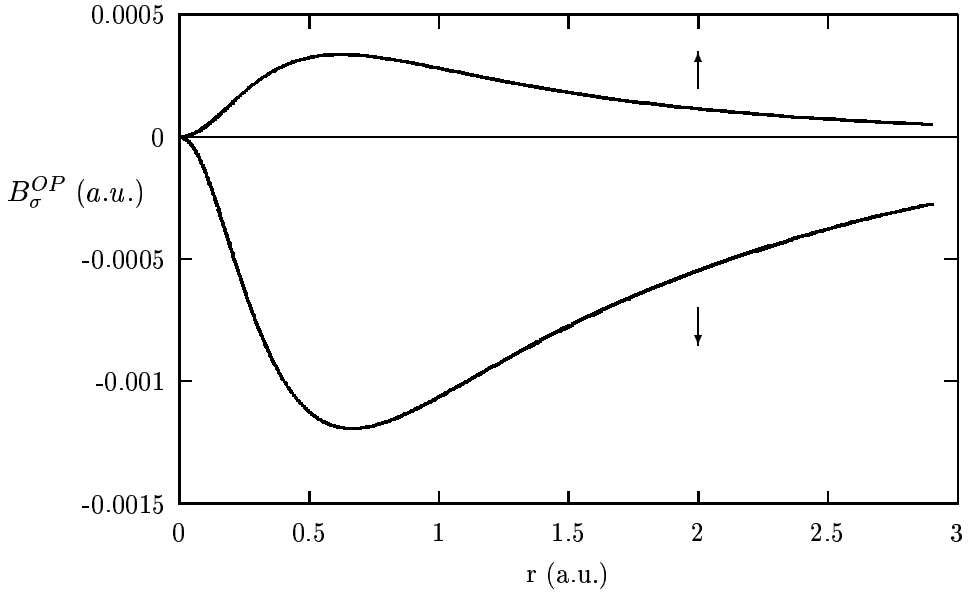

Figure 9: The OP potential term B_σ^{OP} for bcc-Fe as calculated by the self-consistent FP-OP-SPR-KKR.

[4] M. S. S. Brooks and P. J. Kelly, Phys. Rev. Letters **51**, 1708 (1983).

[5] R. Feder, F. Rosicky, and B. Ackermann, Z. Physik B **52**, 31 (1983).

[6] P. Strange, J. B. Staunton, and B. L. Gyorffy, J. Phys. C: Solid State Phys. **17**, 3355 (1984).

[7] A. H. MacDonald and S. H. Vosko, J. Phys. C: Solid State Phys. **12**, 2977 (1979).

[8] M. V. Ramana and A. K. Rajagopal, Adv. Chem. Phys. **54**, 231 (1983).

[9] G. Vignale, in *Current Density Functional Theory and Orbital Magnetism*, Vol. 337 of *Nato ASI Series, Series B*, edited by E. K. U. Gross and R. M. Dreizler (Plenum Press, NewYork, 1995), p. 485.

[10] M. S. S. Brooks, Physica B **130**, 6 (1985).

[11] O. Eriksson, B. Johansson, and M. S. S. Brooks, J. Phys.: Condensed Matter **1**, 4005 (1989).

[12] A. K. Rajagopal and J. Callaway, Phys. Rev. B **7**, 1912 (1973).

[13] G. Vignale and M. Rasolt, Phys. Rev. Letters **59**, 2360 (1987).

[14] G. Vignale and M. Rasolt, Phys. Rev. B **37**, 10685 (1988).

[15] G. Vignale and M. Rasolt, Phys. Rev. Letters **62**, 115 (1989).

[16] H. Ebert, M. Battocletti, and E. K. U. Gross, Europhys. Lett. **40**, 545 (1997).

[17] T. Huhne, Master's thesis, University of Munich, 1997.

[18] P. Söderlind *et al.*, Phys. Rev. B **45**, 12911 (1992).

[19] M. B. Stearns, in *Magnetic Properties of 3d, 4d and 5d Elements, Alloys and Compounds*, Vol. III/19a of *Landolt-Börnstein, New Series*, edited by K.-H. Hellwege and O. Madelung (Springer, Berlin, 1987).

[20] H. Ebert and M. Battocletti, Solid State Commun. **98**, 785 (1996).

[21] K. Capelle and E. K. U. Gross, Phys. Rev. Letters **78**, 1872 (1997).

[22] H. Ebert, H. Freyer, and M. Deng, Phys. Rev. B **56**, 9454 (1997).

Scientific Highlights

This node was part of two intensive collaborations, one with the group of Prof. Schwarz (TU Wien) the other with Prof. Koenig and Dr. Katan (University Rennes I and CNRS.)

Former PhD Students from Prof. Schwarz' group, Dr. Margl and Dr. Nusterer visited the IBM Zurich Research Laboratory on a regular basis for several years, and spent the larger fraction of their work time at the Zurich Laboratory. Dr. Sarnthein from the Vienna group and Dr. Katan (Rennes) spent several extended periods in Zurich. The Swiss Office for Education and Science supported, under the umbrella of the Network, several coordinative and collaborative visits of Dr. Blöchl in Vienna, and the participation of Dr. Andreoni, Dr. Blöchl, Dr. Meijer and Prof. Petrilli from our Institution at the network conference in Schwäbisch Gmund.

The common theme of our collaborations have been applications of the Projector Augmented Wave (PAW) method, which has been developed by Dr. Blöchl at the Zurich Research Laboratory. The PAW method is a new electronic structure method, which is particularly suited to study large molecules and complex materials with high accuracy. This approach has been implemented into an ab-initio molecular dynamics approach, also called the Car-Parrinello method after its inventors, which allows to study the atomic motion in time at finite temperatures.

The collaborations have been particularly useful to gain experience in a number of different fields, ranging from materials science to chemistry, from electronic and optical properties to catalysis. The expertise of the Vienna group with the LAPW method, which is considered one of the most accurate electronic structure methods, helped to prove accuracy and reliability of the PAW method. We find, that the expertise build up in these studies is highly valuable for addressing problems of technological interest.

In the following, I will briefly summarize our main collaborative activities:

Dynamical properties of organometallic sandwich compounds [1,2,6]

Sandwich compounds are a class of synthetic materials that are presently reaching fame as polymerization catalysts. We studied two members of this class, ferrocene and beryllocene. Though they themselves do not exhibit catalytic behavior, they exhibit extreme dynamical behavior, ranging from a wheel like rotation of aromatic rings to full fluxionality between two binding modes. These substances have been widely studied, and allowed to benchmark our dynamical calculations by comparing with experiments. Furthermore, our calculations offered a new interpretation of the measured findings in the case of ferrocene. These studies have been the basis for a number of investigations of homogeneous catalytic processes, carried out at IBM Research Laboratory in collaboration with the ETH Zurich and at the University of Calgary, CA.

Diffusion in the super-ionic conductor Li_3N [5]

Li_3N exhibits large ion conductivities, which has been widely studies because of potential applications in solid state batteries. We have investigated the Li ion diffusion mechanisms at finite temperatures. We found that the rate is mostly controlled by the number of Li-vacancies, while the diffusion process itself is very rapid.

Adsorption of Methanol and Water in Zeolites [3,4,7,9,11]

Zeolites are solid state catalysts used widely in petrochemistry. One of the key problems of zeolite chemistry is how polar molecules interact with acid sites giving rise to catalytic activity. This problem has not been able to resolve unambiguously either by theory nor experiment. We brought to bear all the advantages of our methodology, treating the full crystal structure and not isolated fragments, including electron correlations through density functional theory, and by monitoring the dynamics at finite temperature and in "real" time. On the hand of a prototypical zeolite, we found that the adsorption is strongly coverage dependent: Proton transfer from the acid site to the adsorbed molecule, which is often responsible for catalytic activity, occurs only at larger coverages. These findings provide immediate explanation of puzzling observations of catalytic processes in zeolites. We verified our results by comparing with measured i.r. spectra. The findings have recently been reproduced by other groups for a number of different zeolites.

Electric field gradient calculations with the PAW method [14]

Nuclear probes such as Mössbauer spectroscopy and NMR are particularly sensitive to the electronic wave functions near the nucleus. It has been shown that it is particularly difficult to obtain accurate theoretical predictions for those quantities, because most electronic structure methods approximate the wave function in the relevant region. Dr. Blaha and Prof. Schwarz have been among the pioneers of the calculation of electric field gradients. Together with Prof. Petrilli (Universidade de Sao Paolo and visiting scientist at the IBM Zurich Research Laboratory) we made extensive numerical tests and comparisons with measured and other calculated results. Not only was the comparison with experiments matching the experimental error bars, but also the agreement between the PAW and LAPW methods exceeded the discrepancy from experiment. This opens, for the first time, the possibility to use these quantities for a test of the underlying approximations, such as the choice of the density functionals.

Phase transitions of charge transfer molecular compounds [6,10,12,13]

Charge transfer molecular compounds exhibit a rich phase diagram of electronic and structural phase transitions. For two representative crystals, we investigated the dynamical properties of the molecules and the interactions between the molecules in the low and high symmetry structures. Model parameters required for investigations of the phase transition itself have been derived from our calculations.

References

1. "Finite temperature Characterization of ferrocene from First-Principles Molecular Dynamics"
   P. Margl, K. Schwarz, and P.E. Blöchl, J. Chem. Phys. 100, 8194-8203 (1994)

2. "Dynamics of Beryllocene",
   P. Margl, K. Schwarz, P.E. Blöchl, J. Chem. Phys. 103, 7422-7428 (1995)

3. "Interaction of a Zeolite Acidic Site with Methanol",
   E. Nusterer,P.E. Blöchl and K. Schwarz, Angew. Chem. Int'l Ed. Engl. 35, 175-177 (1996)

4. "Struktur und Dynamik von Methanol in einem Zeolithen",
   E. Nusterer, P.E. Blöchl and K. Schwarz, Angew. Chem. 108, 187-189 (1996)

5. "Ab-Initio Molecular-Dynamics study of diffusion and defects in Solid Li_3N",
   J. Sarnthein, K. Schwarz and P.E. Blöchl, Phys. Rev. B 53, 9084 (1996)

6. "First Principles Molecular Dynamics Simulations for Neutral and Radical Anion of p-Chloranil",
   C. Katan, P.E. Blchl, P. Margl and C. Koenig, Phys. Rev. B 53, 12112 (1996).

7. "Interaction of Water and Methanol with a Zeolite at High Coverages",
   E. Nusterer, P.E. Blöchl and K. Schwarz, Chem. Phys. Lett. 253,448 (1996).

8. "Ab-Initio Molecular Dynamics with the Projector Augmented Wave Method",
   P.E. Blöchl, P. Margl und K. Schwarz, in "Chemical Applications of Density Functional Methods", B.B. Laird, R.B. Ross and T. Ziegler (eds.) (American Chemical Society, Washington D.C. 1996), p.54

9. "Ab-initio Molecular Dynamics Calculations to Study Catalysis",
   K. Schwarz, E. Nusterer, P. Margl and P.E. Blöchl, Int'l J. Quantum Chem. 61, 369 (1997)

10. "Ab-initio calculations of one-dimensional band structures of mixed-stack molecular crystals",
    C. Katan, C. Koenig and P.E. Blöchl, Solid State Comm. 102, 589 (1997)

11. "First-principles molecular dynamics study of small molecules in zeolites",
    K. Schwarz, E. Nusterer and P.E. Blöchl, submitted.

12. "Electronic structure calculations and molecular dynamics simulations of mixed-stack charge-transfer complexes",
    C. Katan, C. Koenig, P.E. Blöchl to be published in Biuletyn Instytutu Chemii Fizycznej i Teoretycznej Politechniki Wroclawskiej 4, (1997) (ISSN 1426-36-96)

13. "First principles investigations of a "quasi-1-dimenional" charge transfer molecular crystal: TTF-2,5Cl_2BQ",
    C. Katan, C. Koenig, P.E. Blöchl, to be published in Comp. Mater. Sci.

14. "Electric Field Gradient Calculations using the Projector Augmented Wave method", H.M. Petrilli, P.E Blöchl, P. Blaha and K. Schwarz, submitted to Phys. Rev. B.

Highlights of Rennes-Zürich Collaboration

C. Katan, C. Koenig and P. E. Blöchl*

Groupe Matière Condensée et Matériaux, Université Rennes-1, Campus de Beaulieu, 35042 Rennes-Cedex, France

**IBM Research Division, Zürich Research Laboratory, CH-8803 Rüschlikon, Switzerland*

This collaboration has been initiated 3 years ago by a Joint Project between IBM Zürich Research Laboratory and University of Rennes. It started with the training of C. Katan (young researcher) in the Projector Augmented Wave (PAW) method developped by P.E. Blöchl and was pursued with a work on the electronic and dynamical properties of molecular charge transfer compounds. C. Katan spent in total 3 months at IBM-Zürich, one of them having been supported by the Network. The publications cited below acknowledge this support.

Charge transfer salts are molecular compounds which exhibit a dazzling variety of phase transitions which can be driven by pressure, temperature, photoirradiation,... They exhibit features ranging from zero to three dimensions and are an ideal ground for fundamental studies which may be useful to understand materials of technological interest such as organic magnets, materials for light emmiting diodes, superconductors, dyes and conducting polymers.

In our quest to obtaining a detailed microscopic understanding of these materials and their transitions, we selected two salts showing a *neutral to ionic* transition: TTF-CA which is the prototypical complex for these transitions and TTF-2,5Cl_2BQ which is less cpu demanding. We first studied all three isolated molecules. The vibrational spectra depending on charge of CA allowed us to make contact with experiments that deduce the ionicity of the crystal from I.R. and Raman spectra [1]. Then we investigated the 1D properties of the crystalline high and low symmetry phases [2, 3, 4]. In particular we got a clear understanding of the tight relation between symmetry breaking and charge transfer increase. At last, we analyzed the 3D interactions combining our ab-initio calculations with a simple tight binding model. Ab-initio values for the charge transfer and the hopping integrals have been derived and their nature has been elucidated.

We derived also a set of parameters that are essential for models allowing to derive a consistent description of the phase transition from which complex nonlinear excitations can be elucidated.

References

[1] C. Katan, P.E. Blöchl, P. Margl and C. Koenig, Phys. Rev. B, **53**, 12112 (1996)

[2] C. Katan, C. Koenig, and P. Blöchl, Solid State Communications, **102**, 589 (1997) and IBM Research Report RZ 2879 (1996)

[3] C. Katan, C. Koenig and P. E. Blöchl, Biuletyn Instytutu Chemii Fizyczne Ji Teoretycznez Politechniki Wroclawskiej (ISSN 1426-36-96), Special issue N° 4 (1997)

[4] C. Katan, C. Koenig, and P. Blöchl, Computational Materials Science, to be published .

Scientific Highlights

During the last few years we have continued our work on developing and applying methods for electronic-structure calculations. Our main emphasis has been on quasi-one-dimensional materials, i.e., chain compounds, where we assume that treating a single, isolated, infinite molecule is a good approximation. To this end we apply a first-principles method we have developed ourselves.

Being a relatively small group our interactions with the colleagues in the network have been somewhat limited. On the other hand, the availability of various types of expertise within the network has been very valuable for our work, as shall be demonstrated below.

During her stay in Konstanz, Catia Arcangeli worked on implementing a generalized-gradient approximation for treating exchange and correlation effects within the density-functional formalism. This should replace the local-density approximation that we so far had been using but which we found could not describe the properties of the systems of our interest correctly. Thus, in particular for hydrogen-bonded systems (that are relevant for a number of biological systems) our local-density calculations gave results that were in wild conflicts with experimental information. It is believed that this can be improved by applying the generalized-gradient approximation. Through the network it was possible for Catia Arcangeli to participate in the Ψ_k network workshop 'Quantum Theory of Solids: Improved Density Functionals' in Århus, June 1994. This was a very convenient opportunity for us to learn about the generalized-gradient approximations. At the moment this work is being continued through studies of proton transport in α-helices that is done in a collaboration with Iris Howard, University of Texas.

Sergei Simak, University of Rennes, visited us for two weeks during December 1994, also made financially possible by the network. Sergei Simak worked on organic molecular crystals, and it was valuable to interchange information and explore whether a joint project could be established. Some calculations on some molecules were done using our code, but ultimately it was decided by the group in Rennes instead to use the code by Peter Blöchl for these studies.

Finally, the network made it possible for Karla Schmidt and myself to participate in the network conference in Schwäbisch Gmünd, September 1996. This conference was very useful and gave actually the inspiration to our only paper that is the direct outcome of our participation in the network.

Our work has continuously been inspired by the input from other work, where the Ψ_k newsletter has been a very important source of information. Of basic contributions to the field of electronic-structure calculations we mention the following two that also should have impacts on the work of the other participants of the network:

We have implemented a method for calculating forces within our full-potential LMTO method for helical polymers. This method includes all terms that correct for approximate eigenfunctions and approximate potentials, and is unique in taking care of the separation of space into muffin-tin spheres and the interstitial region, also for very open systems where about 50% of the valence electrons are found in the interstitial region. Furthermore, through the scheme of our paper below we can without noteworthy additional complications treat metallic systems where the orbital occupancies no longer are constants. We are currently testing a molecular-dynamics program that subsequently will be applied to various polymeric systems, first of all the conjugated polymers.

In many cases the polymeric systems possess deviations from pure periodicity. This may be due to extra charges or to structural distortions. Since these defects may be quite delocalized it is very difficult to treat them theoretically. On the other hand, their existence is important for a number of properties of the materials, and it is therefore highly desirable to be able to obtain results also from theoretical calculations. A standard approach is to apply model Hamiltonians where the parameters may be obtained either from exact calculations on some simplified structures or from experimental information. During the last years we have shown that there is a very simple scheme that can be used to give highly accurate information on the energies of the localized orbitals as long as the defect is extended and as long as a single-particle model is applicable. When the latter not is the case, one needs to include many-body effect as, e.g., contained within the (extended) Hubbard model. Here, however, it is not obvious how to determine the parameters of the model Hamiltonian from theory. This is first of all the case for fairly delocalized electrons for which a separation into atomic components is non-trivial. We have therefore developed a method that relies on the so-called constrained-density-functional method and that can be used in calculating the values of the Hubbard parameters without being strongly dependent on the ambiguity of separating the orbitals into atomic components. The method has been tested on some simple, finite and infinite, systems, and is currently being applied on some carbon-based polymeric materials.

Publication:

M. Springborg, R. C. Albers, and K. Schmidt: Fractional occupancies and temperature in electronic-structure calculations, Phys. Rev. B, January 15th, 1998.

Node: **Stuttgart/Belfast**

Highlights of Collaborations on Large Systems

M. W. Finnis
Atomistic Simulation Group, School of Mathematics and Physics,
The Queen's University of Belfast, Belfast BT7 1NN, Northern Ireland
WWW: http://titus.phy.qub.ac.uk

Introduction

The bonding at interfaces in materials is of wide ranging scientific and practical importance, and has received considerable attention from our electronic structure community. One area of research reported by the Cambridge group has been to understand the mechanism of sliding of grain boundaries, and the embrittling effect of impurities, focussing on the effect of Ga at grain boundaries in Al. Another focus of interest, reported here, has been the intrinsic adhesion of metals to oxides. The importance of the interaction of metals with oxides is ubiquitous in industry, medicine, transport and the home. Protective aluminium oxide scales are a blessing, iron oxide formation is a curse. Medical implants depend on the adherence and longevity of metal-oxide bonds. We are pursuing a programme of basic research in order to understand better the nature of the bonds involved, which do not fit into the neat categories of ionic, covalent or metallic. The network has supported interactions between the Stuttgart node (M.W.Finnis prior to 1.9.95), Belfast (M.W.Finnis since 1.9.95), Berlin (M. Scheffler), Cambridge (M.C. Payne; also V.Y. Milman now with MSI/Biosym) and Keele (M.J.Gillan). The publications cited below acknowledge this support.

The model system Nb/α-Al_2O_3 was chosen for the first *ab initio* study of a metal-alumina interface in which all atomic positions were relaxed to minimise the total energy. The reasons for this choice were partly experimental. It is an interface which can be prepared to a high degree of perfection at the atomic scale, which has enabled detailed studies by high-resolution electron microscopy. The experimental studies suggested a model of the Nb(111)/α-Al_2O_3(0001) interface which has an intriguing construction. The first two layers of Nb atoms appeared to occupy those sites adjacent to the interfacial plane of oxygen atoms which would have been occupied by Al atoms if the Al_2O_3 crystal structure were extended beyond the interface.

Calculations

The calculations, which were done in Stuttgart, are described in detail in our recent publication [1]. We used the pseudopotential/plane wave method developed mainly in the Cambridge group and now commercialised by MSI/Biosym in the form of the CASTEP code. We built on previous

experience in the Keele group, where the structure and energies of α-Al_2O_2 surfaces had been calculated. These calculations were based on a slab of Al_2O_3 containing three layers of oxygen and fifteen atoms altogether, with an equal thickness of vacuum between the (0001) surfaces. Compared to the calculations for boundaries in Si and Al, larger basis sets are needed to describe the bonding in oxides and transition metals, which means that so far only the simplest systems have been tackled.

Preliminary calculations were made with a monolayer of Nb replacing the surface layer of Al. Three different symmetry sites for the Nb were investigated, in each case doing a static relaxation of the total energy. Site A is the observed site which continues the bulk lattice, where the Nb sits in a triangular hollow in the oxygen plane, Sites B and C are also triangular hollows, which differ from A by being vertically above an Al atom in an octahedal site within the plane below. The corresponding octahedral site below the A site is empty.

These calculations were followed by adding further layers of Nb, up to eight altogether, filling the gap between the slabs of Al_2O_3. Finally the effect was calculated of replacing the interfacial layer of Nb with Al.

Results for Nb/α-Al_2O_3

The monolayer calculations showed that when Nb is in site A the energy of the system is lowest. In this case the relaxations of the atomic positions are also very small. By contrast, sites B and C are much higher in energy, by more than 3eV, and the relaxations are very pronounced. We observe that when the Nb is on sites B and C there is a strong repulsion between it and the Al atom below it. This is an ionic repulsion. We showed this by plotting the charge density for different energies, which revealedf that the Nb is in the form of an Nb^{3+} ion, a non-spherical ion with an occupied d-orbital perpendicular to the surface.

With five to eight layers of Nb in a multilayer configuration the situation is rather different. There is still charge transfer to the surface layer of oxygen, enabling it to have a full shell of p-electrons. However, the second layer of Nb participates in this bonding too. The overlap of the Nb d-band with the oxygen 2p-band gives rise to a strong hybridisation which does not happen in the monolayer case. Details of the electronic structure are altered very significantly within the Nb even four layers from the interface; notably there is a prominent resonance above the Fermi energy. The Fermi energy itself lies 3eV above the top of the valence band, about half the distance found with the self-consistent tight binding approach. This result is similar to that of other workers who have made calculations on interfaces of Ag, Ti and Al on MgO, in which the Fermi energy is 2.0-2.3eV above the top of the valence band in each case.

The Nb layers at the interface relax quite strongly as a result of the competition of the first two layers of Nb for bonding with the oxygen. The first two layers of Nb pinch together by 0.04nm compared to their bulk spacing. This is just within range of what should be detectable by high resolution transmission electron microscopy, but it has not yet been investigated at the required resolution. When we replace the interfacial layer of Nb by Al, the relaxation is much reduced - it is as if the second Nb layer has given up the competition for O in the presence of the more electropositive Al.

From our predicted atomic positions our colleague G. Moebus in Stuttgart was able to simulate electron microscope images. A surprising result of this was that the difference between an Al-terminated and an O-terminated interface would only just be within the limit of experimental detection by this technique. Other methods, however, such as electron energy loss spectroscopy have been applied which strongly suggest that the Nb termination is the actual one (J. Bruley, private communication).

Conclusions and other issues

We have demonstrated the usefulness of pseudopotential calculations for studying metal-ceramic interfaces. The nature of the bonding is complicated and different for a monolayer and a multilayer. Relaxations of the atomic positions, especially in metastable equilibrium geometries, can be very large. The first results of this collaboration are set in the context of other theories and models of metal-ceramic bonding in ref. [2].

Another issue is to try to find simpler models which describe either the atomic interactions or the electronic structure of such interfaces. We have recently made developments of the tight-binding model to embrace polarisable ionic crystals (Finnis *et al* to be published) which we plan to pursue further in the Belfast group in collaboration with Dr. Polatoglou's group in Thessaloniki. Real interfaces involve imperfections, defects and roughness, which must affect adhesive energies and other properties. However, with our *ab initio* methods the simulation of all but very simple, atomically flat and coherent, systems is too computationally demanding and there will always be problems for which this remains the case. Classical models, which are computationally even simpler than tight-binding, such as introduced in our collaboration with Berlin [3], may also prove useful.

Advances in ab initio methods and computer hardware since the start of the PSIK project have been so great that we are able to return to the direct calculation of adhesion energies of metals on alumina, which was practically impossible at the beginning of the project. Experimental interest in adhesion of metals to sapphire remains high, as witnessed by a recent(December 97) issue of Physical Review Letters [4], so future theoretical work in the area is sure to be welcome.

References

[1] C Kruse, MW Finnis, JS Lin, VY Milman, MC Payne, A De Vita and MJ Gillan, First principles study of the atomistic and electronic structure of the Niobium/α-Alumina(0001) interface. *Phil. Mag. Lett.* **73** 377-383 (1996)

[2] MW Finnis, Review article: The theory of metal ceramic interfaces, *J. Phys.: Condens. Matter* **8** 5811-5836 (1996).

[3] MW Finnis, R Kaschner, C Kruse, J Furthm—ller and M Scheffler, The interaction of a point charge with a metal surface: theory and calculations for (111), (100) and (110) aluminium surfaces *J. Phys.: Condens. Matter* **7** 2001-2019 (1995).

[4] G Song, A Remhof, K Theis-Bröhl and H Zabel, Extraordinary adhesion of niobum on sapphire substrates *Phys. Rev. Lett.* **79** 5062-5065 (1997)